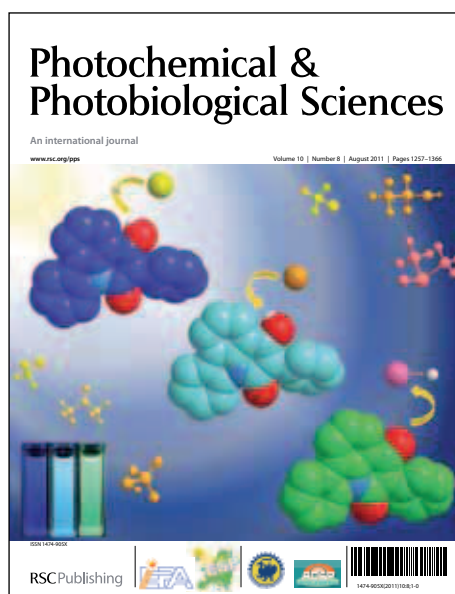


Photochemical & Photobiological Sciences

Accepted Manuscript

This article can be cited before page numbers have been issued, to do this please use: J. R. Vaidya, M. Godumala, B. Shanigaram, A. R. Manda, S. Balasubramanian, P. Singh, R. Srivastava and B. Kotamarthi, *Photochem. Photobiol. Sci.*, 2013, DOI: 10.1039/C3PP50284H.



This is an *Accepted Manuscript*, which has been through the RSC Publishing peer review process and has been accepted for publication.

Accepted Manuscripts are published online shortly after acceptance, which is prior to technical editing, formatting and proof reading. This free service from RSC Publishing allows authors to make their results available to the community, in citable form, before publication of the edited article. This *Accepted Manuscript* will be replaced by the edited and formatted *Advance Article* as soon as this is available.

To cite this manuscript please use its permanent Digital Object Identifier (DOI®), which is identical for all formats of publication.

More information about *Accepted Manuscripts* can be found in the [Information for Authors](#).

Please note that technical editing may introduce minor changes to the text and/or graphics contained in the manuscript submitted by the author(s) which may alter content, and that the standard [Terms & Conditions](#) and the [ethical guidelines](#) that apply to the journal are still applicable. In no event shall the RSC be held responsible for any errors or omissions in these *Accepted Manuscript* manuscripts or any consequences arising from the use of any information contained in them.

Design and Synthesis of Novel Anthracene Derivatives as n-type Emitters for Electroluminescent Devices: A Combined Experimental and DFT Study

G. Mallesham,^{a,b} S. Balaiah,^b M. Ananth Reddy,^{a,b} B. Sridhar,^{*c} Punita Singh,^d Ritu Srivastava,^{*d,e} K. Bhanuprakash^{*b,e} and V. Jayathirtha Rao^{*a,e}

^a Crop Protection Chemicals Division, ^b Inorganic and Physical Chemistry Division,

^c Laboratory of X-Ray Crystallography, Indian Institute of Chemical Technology, Hyderabad 500007, India

^d Organic Electronics, National Physical Laboratory, New Delhi, India

^e National Institute for Solar Energy, New Delhi, India

Keywords: Organic light emitting devices, Anthracene-oxadiazole derivatives, Emitting and Electron-transport materials, DFT calculations, Electroluminescence.

Corresponding author: jrao@iict.res.in

Abstract

Six novel anthracene-oxadiazole derivatives, **4a** (2-(4-(anthracen-9-yl)phenyl)-5-p-tolyl-1,3,4-oxadiazole), **4b** (2-(4-(anthracen-9-yl)phenyl)-5-(4-tert-butylphenyl)-1,3,4-oxadiazole), **4c** (2-(4-(anthracen-9-yl)phenyl)-5-(4-methoxyphenyl)-1,3,4-oxadiazole), **8a** (2-(4-(anthracen-9-yl)phenyl)-5-m-tolyl-1,3,4-oxadiazole), **8b** (2-(3-(anthracen-9-yl)phenyl)-5-(4-tert-butylphenyl)-1,3,4-oxadiazole) and **8c** (2-(3-(anthracen-9-yl)phenyl)-5-(3,4,5-trimethoxyphenyl)-1,3,4-oxadiazole) have been synthesized, characterized for usage as emitters in organic light emitting devices (OLEDs). They show good thermal stability (T_d , 297–364 °C) and glass transition temperatures (T_g) in the range of 82–98 °C as seen from the thermo gravimetric analysis and differential scanning calorimetric studies. Solvatochromism phenomenon using UV-Vis absorption and fluorescence spectroscopy and electrochemical properties have been studied in detail. TD-DFT calculations have been carried out to understand the electrochemical and photo physical properties. The spatial structures of **4b** and **8c** are further confirmed by X-ray diffraction analysis. Un-optimized non-doped electroluminescent devices were fabricated using these anthracene derivatives as emitters with following the device configuration: ITO (120 nm)/ α -NPD (30 nm)/**4a-4c** or **8a-8c** (35 nm)/BCP (6 nm)/Alq₃ (28 nm)/LiF (1 nm)/Al (150 nm). Among all the six compounds, **8a** displays maximum brightness of 1728 cd m⁻² and current efficiency 0.89 cd A⁻¹. Furthermore, **8a** as an electron transporter exhibited superior performance (current efficiency is 11.7 cd A⁻¹) than the device using standard Alq₃ (current efficiency is 8.69 cd A⁻¹) demonstrating their high potential for employment in OLEDs. These results indicate that the new anthracene-oxadiazole derivatives could play an important role in the development of OLEDs.

1. Introduction

Organic light-emitting diodes (OLEDs) have received considerable attention in both scientific and commercial applications since the pioneering work by Tang and VanSlyke in 1987

because of their characteristic low driving voltage, high brightness, full-color emission, fast response time, wide viewing angle and self-emitting properties.^{1,2} Extensive research has been carried out to promote OLEDs into commercial applications as flat-panel displays and solid-state lighting resources due to their low cost.^{3,4} OLEDs have been successfully applied in mobile phones, computers, car stereos, digital cameras,⁵ wrist watches and white solid-state lighting etc.^{6,7} The search for new and efficient emitting materials and charge transport layers remains as one of the most active areas in this field.^{8,9} While bringing out efficient devices is one challenge, understanding the interactions, properties due to substitution, geometry and packing of the molecules in the solid state is another. The latter would help us not only to improve the device efficiency but also give us a more detailed insight into the mechanism of OLED.

The basic structures of the OLED, which have been widely reported in the literature are the multi layer fluorescent emitters and phosphorescent organic light emitting devices (PHOLEDs).^{10,11} Generally in an OLED, three layers such as hole transport layer (HTL), an emitting layer (EML) and an electron transport layers (ETL) are deposited in between anode and cathode with each layer having their own function.¹² In the multi layer fluorescent emitters and PHOLEDs deposition of different layers provides complexity and also increases the cost of the mass production of OLEDs.⁹ To reduce the complexity, overall cost and to increase the extent of OLED commercialization, several organic light-emitting materials possessing electron or hole transporting characteristics or even having both properties in a single molecule are being developed, such that their devices can be simplified to a double or even single-layer device architecture.¹³ The major drawbacks in the doped devices (PHOLEDs) are that the electrochemiluminescence (ECL) properties including color purity are extremely sensitive to the dopant concentration (usually <5%)^{14,15} and triplet-triplet annihilations.^{16,17} Precise control of the dopant concentration using vacuum evaporation or spin coating methods is not an easy task and to prevent exothermic reverse energy transfer in PHOLEDs materials with high triplet energy than the dopant are required.^{18,19} In this regard, it is a good strategy to develop non doped OLEDs based on small molecules with

charge transporting abilities to decrease complexity and cost and to increase existing possibilities for commercialization of OLEDs. In addition, small organic molecules are also having other advantages like easy synthesis, purification and analysis over polymers and inorganic compounds.

Full-color displays require three primary colors (red, green and blue) of relatively equal stability, efficiency and color purity. Among these, a wide range of efficient green and red-emitting devices have been reported.²⁰ However, blue-emitting devices remain relatively less explored due to their intrinsic characteristics such as wide band-gap and low highest occupied molecular orbital (HOMO) energy level, which make it hard to inject charges into the emitting layer.^{21,22} Therefore the development of blue-emitting diodes having more stability and good color purity with longer life times and high efficiency especially with non doped device architecture has become a test bench in the recent years. Many types of blue light emitting materials have been investigated, such as derivatives of anthracene,^{23,24} pyrene,^{25,26} fluorene,^{27,28} spirofluorene,²⁹ triarylamine,^{30,31} carbazole,^{32,33,34} and phenanthrene³⁵ etc. Among these, anthracene has been widely used as a building block to produce blue emitters due to its high photoluminescence efficiency in blue region, high carrier mobility and better hole-injection ability, wide band gap (~3.90 eV),³⁶ structural rigidity, excellent thermal stability for better morphology and easy to modify at 9 and 10 positions of the anthracene moiety. In continuation of our research in the development of OLED materials here we present new series of anthracene derivatives which show promising properties.^{37,38,39}

In this contribution, we have designed and synthesized a series of six small organic molecules, **4a-4c** and **8a-8c** (Scheme 1 and 2) with anthracene core and oxadiazole moiety as electron transporter, which are connected through phenyl spacer with *para* and *meta* linkage. The introduction of oxadiazole moiety enhances electron transporting capability because of two withdrawing C=N groups and also facilitates in improving thermal stability for better morphology. Thermal, electrochemical and photo physical properties for all six compounds are studied in detail. Solid state structure for compounds **4b** and **8c** are

determined by single crystal X-ray diffraction studies. TD-DFT calculations are carried out for all the molecules to understand photo physical and electrochemical properties. Un-optimized non-doped electroluminescent devices were fabricated from these anthracene derivatives with the following configuration: ITO (120 nm)/ α -NPD (30 nm)/**4a-4c** or **8a-8c** (35 nm)/BCP (6 nm)/Alq₃ (28 nm)/LiF (1 nm)/Al (150 nm). In addition, a three layer device using **8a** as an electron transport material and iridium complex as emitter was also fabricated.

2. Experimental details

2.1. Measurements and Instruments

All chemicals are reagent/analytical grade and used without further purification. ¹H NMR and ¹³C NMR spectra were recorded on a Bruker Avance (75 MHz) spectrometer in CDCl₃ with TMS as internal standard. Mass spectra were obtained by using electro spray ionization (ESI) ion trap mass spectrometry (ThermoFinnigan, San Jose, CA, USA) were recorded on VG-AUTOSPEC spectrometer. Elemental analyses were performed using a Vario-EL elemental analyzer. UV-Vis absorption spectra were measured using Jasco V-550 spectrophotometer. Steady state fluorescence spectra were recorded using a Spex Fluorolog-3 spectrofluorometer. The fluorescence quantum yields (Φ) were estimated by integrating the fluorescence bands and by using 9,10-diphenylanthracene (DPA) as standard.⁴⁰ The glass-transition temperatures (T_g) of the compounds were measured using differential scanning calorimetry (DSC) under nitrogen atmosphere at a heating rate of 10 °C min⁻¹ using DSC Q200 (TA instruments). The T_g was determined from the second heating scan. Thermo gravimetric analysis (TGA) was performed using a TGA/SDTA 851e (Mettler Toledo) in the temperature range of 33–550 °C under nitrogen atmosphere at a heating rate of 10 °C min⁻¹. Cyclic voltammetric measurements were performed on a PC-controlled CH instruments model CHI 620C electrochemical analyzer. Cyclic voltammetric experiments were performed in 1 mM solution of degassed dry dichloromethane at a scan rate of 100 mV/s using 0.1M tetrabutylammoniumperchlorate (TBAP) as supporting electrolyte. The

glassy carbon was used as working electrode, Ag/AgCl as the reference electrode and platinum wire as the counter electrode. The working electrode surface was first polished with 1 mm alumina slurry, followed by 0.3 mm alumina slurry on a micro cloth. It was then rinsed with milli cure water and also sonicated in water for 5 min. The polishing and sonication steps were repeated twice.

For the ECL studies, Indium-tin oxide (ITO) coated glass substrates with sheet resistance of 20Ω were photo lithographically patterned and cleaned using trichloroethylene, acetone, isopropyl alcohol and de ionized water sequentially for 20 minutes using an ultrasonic bath and dried in flowing nitrogen. Prior to film deposition, the ITO substrates were treated with UV-ozone for 5 minutes. On the substrate, the hole transport layer, emitting layer, hole blocking layer, electron transport layer, electron injecting layer and cathode were deposited sequentially under a high vacuum (1×10^{-5} torr). The deposition rate of organic materials were kept at $1 \text{ \AA} / \text{sec}$ whereas that of LiF was $0.5 \text{ \AA} / \text{sec}$ and Al at $5 \text{ \AA} / \text{sec}$. Thickness of the deposited layers were controlled by a quartz crystal monitor. The cathode was deposited on the top of the structure through a shadow mask. N,N-diphenyl-N'N'-bis(1-naphthyl)-1,1'-biphenyl-4,4'-diamine, (α -NPD) (Sigma Aldrich) was used as a hole transport layer, BCP was used as hole blocking layer, Tris(8-hydroxyquinoline)aluminium (Alq_3) (Sigma Aldrich) was used as electron transport layer, LiF (Merck, Germany) was an electron injection layer and the Al as cathode. The size of each pixel was 3-4 mm. The ECL spectra were measured using an Ocean Optics high resolution Spectrometer (HR-2000CG UV-NIR). The current density-voltage-luminescence (J-V-L) characteristics were measured with a luminance meter (LMT I-1009) and a Keithley 2400 programmable voltage-current digital source meter. All the measurements were carried out at room temperature under ambient conditions.

2.2. Synthesis and characterization (Scheme 1 and 2)

2.2.1. Synthesis of compounds 2 and 6.^{38,41,42} The compounds 5-(4-bromophenyl)-1H-tetrazole (**2**) and 5-(3-bromophenyl)-1H-tetrazole (**6**) were synthesized according to the following procedure. A mixture of 4-bromobenzonitrile (**1**) / 3-bromobenzonitrile (**5**) (10 g, 55.2 mmol), NaN_3 (5.4 g, 82.9 mmol), Bu_3SnCl (26.9 g, 82.9 mmol) in *m*-xylene (150 mL) was refluxed for 24 h under nitrogen atmosphere. The reaction mixture was cooled to room temperature and acidified with 40 mL of 2N HCl. A white solid suspension formed, filtered on Buchner funnel and washed thoroughly with water followed by *n*-hexane to get titled compound as colorless solid.

2.2.2. 5-(4-bromophenyl)-1H-tetrazole (2).^{38,41} Isolated yield: 96 % (12.0 g). mp: 256 °C. ^1H NMR (300 MHz, CDCl_3): δ 8.00 (d, 2H, $J = 8.3$ Hz), 7.69 (d, 2H, $J = 8.3$ Hz). MS (ES+): m/z 225 (M+H)⁺.

2.2.3. 5-(3-bromophenyl)-1H-tetrazole (6).^{38,42} Isolated yield: 95 % (11.9 g). mp: 151 °C. ^1H NMR (300 MHz, CDCl_3): δ 8.25 (s, 1H), 8.05 (d, 1H, $J = 7.2$ Hz), 7.63 (d, 1H, $J = 7.2$ Hz), 7.44 (t, 1H, $J = 7.2$ Hz). MS (ES+): m/z 225 (M+H)⁺.

2.2.4. 2-(4-bromophenyl)-5-*p*-tolyl-1,3,4-oxadiazole (3a).⁴³ To a stirred solution of **2** (8.0 g, 35.5 mmol) in dry pyridine (15 mL), 4-methylbenzoyl chloride (5.1 mL, 39.1 mmol) was added slowly via syringe under nitrogen atmosphere. The reaction temperature was raised to reflux and continued for 6 h, later slowly brought to ambient temperature, and then 20 mL of water was added to precipitate out colorless solid compound. Thus obtained solid was filtered, washed thoroughly with water, dried and purified by silica gel column chromatography using ethyl acetate/ hexane (1:10) as eluent. The obtained solid was further recrystallized from toluene/ *n*-hexane to get **3a** as colorless solid. Isolated yield: 85% (9.5 g). mp: 205 °C. ^1H NMR (300 MHz, CDCl_3): δ 7.98 (d, 4H, $J = 8.3$ Hz), 7.65 (d, 2H, $J = 8.3$ Hz), 7.30 (d, 2H, $J = 8.3$ Hz), 2.44 (s, 3H). ^{13}C NMR (75 MHz, CDCl_3): δ 164.80, 163.50, 142.40, 132.31, 129.72, 128.18, 126.81, 126.20, 122.83, 120.82, 21.61. MS (ES+): m/z 316 (M+H)⁺.

2.2.5. 2-(4-bromophenyl)-5-(4-*tert*-butylphenyl)-1,3,4-oxadiazole (3b).^{18,38} This compound was synthesized according to the procedure similar to that of **3a**, using **2** (8.0 g, 35.5 mmol),

4-tert-butylbenzoyl chloride (8.1 mL, 39.1 mmol) and dry pyridine (15 mL) to get colorless solid. Isolated yield: 79% (10.1 g). mp: 142 °C. ^1H NMR (300 MHz, CDCl_3): δ 7.99-8.01 (m, 4H), 7.65 (d, 2H, J = 8.8 Hz), 7.51 (d, 2H, J = 7.8 Hz), 1.38 (s, 9H). ^{13}C NMR (75 MHz, CDCl_3): δ 164.52, 163.31, 155.14, 132.45, 128.36, 126.93, 126.25, 125.91, 123.27, 121.25, 35.24, 31.38. MS (ES+): m/z 358 (M+H) $^+$.

2.2.6. 2-(4-bromophenyl)-5-(4-methoxyphenyl)-1,3,4-oxadiazole (3c).⁴⁴ This compound was synthesized according to the procedure similar to that of **3a**, using **2** (8.0 g, 35.5 mmol), 4-methoxybenzoyl chloride (5.8 mL, 39.1 mmol) and dry pyridine (15 mL) to get colorless solid. Isolated yield: 83% (9.8 g). mp: 159 °C. ^1H NMR (300 MHz, CDCl_3): δ 8.10 (d, 2H, J = 9.0 Hz), 7.96 (d, 2H, J = 8.0 Hz), 7.64 (d, 2H, J = 8.0 Hz), 6.98 (d, 2H, J = 9.0 Hz), 3.87 (s, 3H). ^{13}C NMR (75 MHz, CDCl_3): δ 163.13, 162.36, 132.32, 128.66, 128.14, 126.09, 123.06, 116.26, 114.47, 55.33. MS (ES+): m/z 331 (M+H) $^+$.

2.2.7. 2-(3-bromophenyl)-5-p-tolyl-1,3,4-oxadiazole (7a). This compound was synthesized according to the procedure similar to that of **3a**, using **6** (8.0 g, 35.5 mmol), 3-methylbenzoyl chloride (5.1 mL, 39.1 mmol) and dry pyridine (15 mL) to get colorless solid. Isolated yield: 72 % (8.1 g). mp: 140 °C. ^1H NMR (300 MHz, CDCl_3): δ 8.22 (s, 1H), 8.07 (d, 1H, J = 7.7 Hz), 8.01 (d, 2H, J = 8.1 Hz), 7.64 (d, 1H, J = 8.1 Hz), 7.42-7.36 (t, 1H, J = 7.7 Hz), 7.30 (d, 2H, J = 8.1 Hz), 2.45 (s, 3H). ^{13}C NMR (75 MHz, CDCl_3): δ 164.72, 162.69, 142.32, 134.29, 130.41, 129.60, 129.38, 126.69, 125.58, 125.14, 122.86, 120.56, 21.48. MS (ES+): m/z 316 (M+H) $^+$.

2.2.8. 2-(3-bromophenyl)-5-(4-tert-butylphenyl)-1,3,4-oxadiazole (7b).³⁸ This compound was synthesized according to the procedure similar to that of **3a**, using **6** (8.0 g, 35.5 mmol), 3-tert-butylbenzoyl chloride (8.1 mL, 39.1 mmol) and dry pyridine (15 mL) to get colorless solid. Isolated yield: 72% (9.2 g). mp: 115 °C. ^1H NMR (300 MHz, CDCl_3): δ 8.25-8.24 (t, 1H), 8.09-8.02 (m, 3H), 7.67-7.63 (dd, 1H, J = 8.3 Hz), 7.52 (d, 2H, J = 8.3 Hz), 7.42-7.37 (t, 1H, J = 8.3 Hz), 1.38 (s, 9H). ^{13}C NMR (75 MHz, CDCl_3): δ 164.77, 162.84, 155.38, 134.40,

130.53, 129.63, 126.84, 125.99, 125.93, 125.33, 123.09, 120.84, 35.08, 31.15. MS (ES+): m/z 358 (M+H)⁺.

2.2.9. 2-(3-bromophenyl)-5-(3,4,5-trimethoxyphenyl)-1,3,4-oxadiazole (7c). This compound was synthesized according to the procedure similar to that of **3a**, using **6** (8.0 g, 35.5 mmol), 3,4,5-trimethoxybenzoyl chloride (9.0 g, 39.1 mmol) and dry pyridine (15 mL) to get colorless solid. Isolated yield: 73 % (10.2 g). mp: 152 °C. ¹H NMR (300 MHz, CDCl₃): δ 8.23-8.22 (t, 1H), 8.08-8.05 (m, 1H), 7.68-7.64 (dd, 1H, *J* = 8.3 Hz), 7.42-7.37 (t, 1H, *J* = 8.3 Hz), 7.29 (s, 2H), 3.97 (s, 6H), 3.90 (s, 3H). ¹³C NMR (75 MHz, CDCl₃): δ 164.63, 163.00, 153.55, 141.21, 134.46, 130.48, 129.44, 125.54, 125.29, 122.91, 118.47, 104.11, 60.87, 56.30. MS (ES+): m/z 391 (M+H)⁺.

2.2.10. 2-(4-(anthracen-9-yl)phenyl)-5-p-tolyl-1,3,4-oxadiazole (4a). To a suspension of **3a** (1.5 g, 4.8 mmol) in dry THF (30 mL), *n*-BuLi (2.6 mL, 5.2 mmol, 2.0M in cyclohexane) was added drop wise at -78 °C (using dry ice-acetone) for 10 minutes. The reaction mixture was stirred for 1 h and then anthrone (0.83 g, 4.3 mmol) which was dissolved in 30 mL of dry THF added to the reaction mixture via syringe at same temperature for 15 minutes. It was stirred at same temperature for 1 h, brought to ambient temperature and continued for 3 h. Excess *n*-BuLi was destroyed using saturated NH₄Cl solution (5 mL). The organic compound was extracted with ethyl acetate (3 x 60 mL), combined organic layers were dried over sodium sulphate and solvent was removed under reduced pressure to get foamy residue. Thus obtained compound was dissolved in acetone (50 mL), conc. HCl (1.0 mL) was added and stirred for 3 h. Then water (20 mL) was added to reaction mixture and extracted the compound with ethyl acetate, washed with brine solution followed by water. Combined organic layers were dried over sodium sulphate and the solvent was removed under reduced pressure. Thus obtained crude compound was purified by silica gel column chromatography using ethyl acetate/ hexane (1:10) as eluent to get product. Thus product was further precipitated using CHCl₃/MeOH (1:4) to get **4a** as colorless solid. Isolated yield: 43% (0.77 g). mp: 236 °C. ¹H NMR (300 MHz, CDCl₃): δ 8.47 (s, 1H), 8.34 (d, 2H, *J* = 7.8 Hz), 8.05 (d,

2H, $J = 7.8$ Hz), 8.01 (d, 2H, $J = 7.8$ Hz), 7.61 (d, 4H, $J = 8.8$ Hz), 7.44-7.41 (t, 2H, $J = 7.8$ Hz), 7.35-7.32 (t, 4H, $J = 7.8$ Hz), 2.46 (s, 3H). ^{13}C NMR (75 MHz, CDCl_3): δ 142.61, 141.94, 132.05, 131.38, 129.92, 129.75, 129.66, 128.93, 128.44, 127.16, 126.93, 126.87, 126.26, 125.71, 125.12, 123.35, 121.34, 21.70. FTIR (KBr, cm^{-1}): 3043, 2960, 1611, 1491, 1066, 731. MS (ES⁺): m/z 413 (M+H)⁺. Anal. Calcd (%) for $\text{C}_{21}\text{H}_{20}\text{N}_2\text{O}$: C 84.44, H 4.89, N 6.79. Found: C 84.42, H 4.90, N 6.78.

2.2.11. 2-(4-(anthracen-9-yl)phenyl)-5-(4-tert-butylphenyl)-1,3,4-oxadiazole (4b). This compound was synthesized according to the procedure similar to that of **4a**, using **3b** (1.5 g, 4.2 mmol), *n*-BuLi (2.3 mL, 4.6 mmol, 2.0M in cyclohexane), anthrone (0.73 g, 3.8 mmol), dry THF 60 (30+30) mL, acetone (50 mL) and conc. HCl (1.0 mL) to get light green solid. Isolated yield: 49% (0.85 g). mp: 210 °C. ^1H NMR (300 MHz, CDCl_3): δ 8.47 (s, 1H), 8.35 (d, 2H, $J = 8.1$ Hz), 8.08 (d, 2H, $J = 9.0$ Hz), 8.01 (d, 2H, $J = 8.1$ Hz), 7.61 (d, 4H, $J = 8.1$ Hz), 7.54 (d, 2H, $J = 9.0$ Hz), 7.44-7.41 (t, 2H, $J = 7.2$ Hz), 7.35-7.32 (t, 2H, $J = 8.1, 7.2$ Hz), 1.39 (s, 9H). ^{13}C NMR (75 MHz, CDCl_3): δ 164.74, 164.31, 155.36, 142.58, 135.38, 132.04, 131.23, 129.86, 128.43, 127.16, 126.93, 126.77, 126.22, 126.06, 125.73, 125.18, 123.23, 121.07, 35.07, 31.10. FTIR (KBr, cm^{-1}): 3050, 2961, 2905, 2866, 1611, 1492, 1063, 843, 729. MS (ES⁺): m/z 455 (M+H)⁺. Anal. Calcd (%) for $\text{C}_{32}\text{H}_{26}\text{N}_2\text{O}$: C 84.55, H 5.77, N 6.16. Found: C 84.53, H 5.78, N 6.15.

2.2.12. 2-(4-(anthracen-9-yl)phenyl)-5-(4-methoxyphenyl)-1,3,4-oxadiazole (4c). This compound was synthesized according to the procedure similar to that of **4a**, using **3c** (1.5 g, 4.5 mmol), *n*-BuLi (2.5 mL, 5.0 mmol, 2.0M in cyclohexane), anthrone (0.79 g, 4.1 mmol), dry THF 60 (30+30) mL, acetone (50 mL) and conc. HCl (1.0 mL) to get light green solid. Isolated yield: 40% (0.70 g). mp: 220 °C. ^1H NMR (300 MHz, CDCl_3): δ 8.50 (s, 1H), 8.35 (d, 2H, $J = 7.9$ Hz), 8.12 (d, 2H, $J = 8.9$ Hz), 8.04 (d, 2H, $J = 7.9$ Hz), 7.62 (d, 4H, $J = 7.9$ Hz), 7.45 (t, 2H, $J = 6.9, 7.9$ Hz), 7.37-7.35 (t, 2H, $J = 6.9, 7.9$ Hz), 7.04 (d, 2H, $J = 8.9$ Hz), 3.91 (s, 3H). ^{13}C NMR (75 MHz, CDCl_3): δ 169.54, 164.02, 142.55, 135.42, 132.08, 131.32, 129.95, 128.73, 128.49, 127.21, 126.89, 126.32, 125.76, 125.21, 123.40, 116.54, 114.56,

55.39. FTIR (KBr, cm^{-1}): 3042, 2957, 2832, 1609, 1493, 1253, 1170, 823, 729. MS (ES⁺): m/z 429 (M+H)⁺. Anal. Calcd (%) for $\text{C}_{29}\text{H}_{20}\text{N}_2\text{O}_2$: C 81.29, H 4.70, N 6.54. Found: C 81.27, H 4.73, N 6.55.

2.2.13. 2-(4-(anthracen-9-yl)phenyl)-5-m-tolyl-1,3,4-oxadiazole (8a). This compound was synthesized according to the procedure similar to that of **4a**, using **7a** (1.5 g, 4.8 mmol), *n*-BuLi (2.6 mL, 5.2 mmol, 2.0M in cyclohexane), anthrone (0.83 g, 4.3 mmol), dry THF 60 (30+30) mL, acetone (50 mL) and conc. HCl (1.0 mL) to get colorless solid. Isolated yield: 36% (0.61 g). mp: 207 °C. ¹H NMR (300 MHz, CDCl_3): δ 8.50 (s, 1H), 8.37 (d, 1H, $J = 7.9$ Hz), 8.15 (s, 1H), 8.03 (d, 2H, $J = 8.3$ Hz), 7.96 (d, 2H, $J = 8.1$ Hz), 7.78-7.73 (t, 1H, $J = 7.7$ Hz), 7.60 (d, 3H, $J = 9.1$ Hz), 7.46-7.41 (t, 2H, $J = 6.8, 7.5$ Hz), 7.36-7.32 (t, 2H, $J = 6.8, 7.5$ Hz), 7.24 (d, 2H, $J = 7.5$ Hz), 2.40 (s, 3H). ¹³C NMR (75 MHz, CDCl_3): δ 164.69, 164.11, 142.07, 140.04, 135.22, 134.42, 131.33, 130.17, 129.69, 129.40, 129.28, 128.48, 127.20, 126.93, 126.38, 126.18, 125.79, 125.20, 124.52, 121.14, 21.68. FTIR (KBr, cm^{-1}): 3045, 2922, 1615, 1494, 1261, 1066, 735. MS (ES⁺): m/z 413 (M+H)⁺. Anal. Calcd (%) for $\text{C}_{21}\text{H}_{20}\text{N}_2\text{O}$: C 84.44, H 4.89, N 6.79. Found: C 84.43, H 4.90, N 6.78.

2.2.14. 2-(3-(anthracen-9-yl)phenyl)-5-(4-tert-butylphenyl)-1,3,4-oxadiazole (8b). This compound was synthesized according to the procedure similar to that of **4a**, using **7b** (1.5 g, 4.2 mmol), *n*-BuLi (2.3 mL, 4.6 mmol, 2.0M in cyclohexane), anthrone (0.73 g, 3.8 mmol), dry THF 60 (30+30) mL, acetone (50 mL) and conc. HCl (1.0 mL) to get colorless solid. Isolated yield: 42% (0.72 g). mp: 204 °C. ¹H NMR (300 MHz, CDCl_3): δ 8.50 (s, 1H), 8.35 (d, 1H, $J = 7.7$ Hz), 8.18 (s, 1H), 8.04-7.97 (m, 4H), 7.77-7.72 (t, 1H, $J = 7.5, 7.7$ Hz), 7.61 (d, 3H, $J = 8.7$ Hz), 7.46-7.41 (t, 4H, $J = 5.7, 8.3$ Hz), 7.37-7.31 (t, 2H, $J = 7.0, 8.3$ Hz), 1.34 (s, 9H). ¹³C NMR (75 MHz, CDCl_3): δ 164.54, 164.05, 155.03, 140.07, 135.23, 134.39, 131.36, 130.20, 129.44, 129.23, 128.49, 127.20, 126.83, 126.40, 126.17, 125.90, 125.79, 125.19, 124.65, 121.21, 35.09, 31.23. FTIR (KBr, cm^{-1}): 3048, 2956, 2864, 1611, 1491, 1265, 842, 730. MS (ES⁺): m/z 455 (M+H)⁺. Anal. Calcd (%) for $\text{C}_{32}\text{H}_{26}\text{N}_2\text{O}$: C 84.55, H 5.77, N 6.16. Found: C 84.55, H 5.78, N 6.17.

2.2.15. 2-(3-(anthracen-9-yl)phenyl)-5-(3,4,5-trimethoxyphenyl)-1,3,4-oxadiazole (8c).

This compound was synthesized according to the procedure similar to that of **4a**, using **7c** (1.5 g, 3.8 mmol), *n*-BuLi (2.1 mL, 4.2 mmol), anthrone (0.67 g, 3.5 mmol), dry THF 60 (30+30) mL, acetone (50 mL) and conc. HCl (1.0 mL) to get colorless solid. Isolated yield: 40% (0.68 g). mp: 232 °C. ¹H NMR (300 MHz, CDCl₃): δ 8.51 (s, 1H), 8.38 (d, 1H, *J* = 7.7 Hz), 8.15 (s, 1H), 8.04 (d, 2H, *J* = 8.5 Hz), 7.79-7.73 (t, 1H, *J* = 7.7, 7.5 Hz), 7.62-7.59 (m, 3H), 7.47-7.42 (t, 2H, *J* = 7.2, 7.5 Hz), 7.37-7.32 (t, 2H, *J* = 6.8, 8.3 Hz), 7.26 (d, 2H), 3.90 (s, 6H), 3.86 (s, 3H). ¹³C NMR (75 MHz, CDCl₃): δ 164.58, 164.38, 153.58, 141.01, 139.89, 135.19, 134.48, 131.19, 130.06, 129.32, 129.19, 128.43, 127.15, 126.29, 126.25, 125.76, 125.23, 124.21, 118.82, 104.02, 60.95, 56.35. FTIR (KBr, cm⁻¹): 3048, 2966, 2939, 2833, 1592, 1496, 1236, 1126, 845, 740. MS (ES⁺): *m/z* 489 (M+H)⁺. Anal. Calcd (%) for C₃₁H₂₄N₂O₄: C 76.21, H 4.95, N 5.73. Found: C 76.22, H 4.96, N 5.71.

2.3 Computational methods

Density functional theory calculations were carried out for the anthracene derivatives to know absorption, HOMO and LUMO values. Ground state geometries of the molecules were obtained at B3LYP/6-311G(d,p) level of theory. Frequency calculations were performed at the same level of theory to ensure the optimized geometries are local minima on the potential energy surface. Time dependant density functional theory was employed for the simulation of absorption spectra using B3LYP/6-311G(d,p) in different solvents (Hexane, CHCl₃ and CH₃OH) using Polarizable Continuum Model (PCM)⁴⁵ as implemented in Gaussian09 software⁴⁶ for better understanding of the excitation. The absorption maxima reported here was the excitation energy taken from vertical S₀-S₁ transition.

3. Results and discussion

3.1 Synthesis

In this contribution, we present the synthesis of six new compounds, namely 2-(4-(anthracen-9-yl)phenyl)-5-p-tolyl-1,3,4-oxadiazole (**4a**), 2-(4-(anthracen-9-yl)phenyl)-5-(4-tert-butylphenyl)-1,3,4-oxadiazole (**4b**), 2-(4-(anthracen-9-yl)phenyl)-5-(4-methoxyphenyl)-1,3,4-oxadiazole (**4c**), 2-(4-(anthracen-9-yl)phenyl)-5-m-tolyl-1,3,4-oxadiazole (**8a**), 2-(3-(anthracen-9-yl)phenyl)-5-(4-tert-butylphenyl)-1,3,4-oxadiazole (**8b**), 2-(3-(anthracen-9-yl)phenyl)-5-(3,4,5-trimethoxyphenyl)-1,3,4-oxadiazole (**8c**), which features anthracene as an emitter, oxadiazole as an electron transporter and phenyl group as spacer and end group to influence thermal, optical and electrochemical properties designed for OLED applications. The synthetic details are illustrated in Scheme 1 and 2. The intermediates **2** and **6** were obtained^{38,41,42} from 4-bromobenzonitrile (**1**), 3-bromobenzonitrile (**5**) upon treating with NaN₃ and Bu₃SnCl in *m*-xylene. The key intermediates **3a-3c** and **7a-7c** were synthesized^{18,38,43,44} upon treatment of **2** and **6** with the corresponding acid chlorides refluxed in dry pyridine. Further, upon metal halogen exchange of **3a-3c** and **7a-7c** by treating with *n*-BuLi followed by addition of anthrone produces corresponding alcohols. Thus obtained alcohols, without further purification were treated with catalytic amount of conc. HCl in acetone to obtain final compounds (**4a-4c**, **8a-8c**). Products were purified by column chromatography followed by recrystallization before spectral characterization. All these compounds are readily soluble in common organic solvents like chloroform, DCM and THF etc. The molecular structures of **4b** and **8c** were further confirmed by single-crystal X-ray diffraction analysis.

3.2. Molecular geometry and crystal structure

The anthracene derivatives **4b** and **8c** were crystallized from CH₃OH/CHCl₃ (1:4) and the single crystal structures determined. Both crystallize into the monoclinic P2₁/c space group. The summary of crystal data and structure refinement details are given in supporting information. The X-ray molecular structures are shown in Fig. 1. In both crystals there are

four independent molecules of anthracene derivatives in the unit cell. The phenyl ring forms a twist angle of 98.9° with the anthracene and oxadiazole is almost in the same plane as the phenyl ring (a twist angle of only -7.0°). Similarly the corresponding twist angles in **8c** are observed to be 70.6° , and 25.8° respectively which is shown in the same figure. The geometrical parameters from B3LYP method are in line with the crystal data. But the dihedral angles from theory are a little deviated from X-ray values which could be attributed to the intermolecular forces in the solid state environment. The anthracene–phenyl connecting C–C bond length C(12)–C(15) is $1.484(3)$ Å and C(13)–C(15) (see Fig. 2 for carbon atom numbering in SI) is $1.497(3)$ Å for **4b** and **8c** respectively which indicates more single bond character giving chance for free rotation.

Crystal structure of **4b** is mainly stabilized by CH π and $\pi\pi$ interactions. Intermolecular stacking interactions (Fig. 2A) are observed between the inversion-related rings of the anthracene moiety (centroid–centroid separation between the inversion-related C15–C28 rings = $3.950(1)$ Å, centroid–centroid separation between C15–C28 and C23–C28 rings = $3.860(1)$ Å and centroid–centroid separation between C16–C21 and C23–C28 rings = $3.884(2)$ Å (see Fig. 2A for carbon numbering in SI) symmetry code (1-x, 2-y, 2-z) and forms a dimer in the crystal packing. The anthracene rings are packed inversely parallel whereas oxadiazole rings are in slip parallel stacking. The crystal structure of **8c** is stabilized by CH π , O, CH π and $\pi\pi$ interactions (Fig. 2B). The intermolecular CH π interaction (C π O = $3.472(3)$ Å, x, 1/2+y, 1/2-z) involving atoms C25 of the anthracene and atom O1 of the oxadiazole forms an infinite helical chain along the b-axis. Intermolecular stacking via $\pi\pi$ interactions are also observed between the symmetry related oxadiazole ring (centroid–centroid separation = $3.838(1)$ Å, symmetry code x, 1/2-y, -1/2+z) and between the oxadiazole and the C1–C6 phenyl ring (centroid–centroid separation = $3.751(1)$ Å, symmetry code = x, 1/2-y, -1/2+z).

3.3. Thermal properties

Thermo gravimetric analysis (TGA) and differential scanning calorimetry (DSC) measurements were performed for all the six new compounds (**4a-4c** and **8a-8c**) to evaluate thermal properties and the results are summarized in Table 1. Representative DSC scans of **4a** and **8a** are shown in Fig. 3 while the further DSC and TGA plots are given in SI. Thermal decomposition temperatures (T_d) corresponding to 5% weight loss of these compounds are in the range of 297–364 °C informing good thermal stability. A key physical parameter which indicates the stability of the amorphous nature of a given material is the glass transition temperature (T_g). In a repeated differential scanning calorimetric (DSC) scan, all the thermograms displayed endothermic baseline shifts owing to glass transitions (T_g) in the range of 82–98 °C without crystallization except for **4c** (142 °C) indicating stable amorphous nature of materials. The melting points of these six compounds are in the range of 204–236 °C. These results reveal that the synthesized compounds are thermally stable with good T_g values to form films with better morphology.

3.4. Electrochemical properties

Cyclic voltammetric measurements were performed to investigate the redox properties of the six (**4a-4c** and **8a-8c**) compounds using three electrode systems. The representative cyclic voltammograms are shown in Fig. 4 and the relevant data is summarized in Table 2. During the anodic voltage sweep all compounds exhibit reversible oxidation and upon cathodic voltage sweep exhibit quasi reversible reduction. The oxidation and reduction onset potentials⁴⁷ are used to calculate the HOMO, LUMO energy values relative to ferrocene as reference using equations $-(4.40 + E_{ox}^{onset})$ ⁴⁸ eV and $-(4.40 + E_{red}^{onset})$ eV, respectively.^{49,50} The HOMO and LUMO energy values are in the range of -5.72 to -5.77 eV and 2.59–2.66 eV, respectively. Small variations in HOMO, LUMO energy values for all compounds indicate similar electronic structure. The computationally calculated HOMO/LUMO energy values are in consistent with experimental values (Table 2, Fig. 5 for **4a** and **8a** and see SI for other data). The electrochemical band gaps and optical band gaps of the synthesized compounds

are in between 3.08–3.18 eV and 3.11–3.17 eV, respectively. The electrochemical band gaps are in good agreement with optical band gaps.

3.5. Photophysical properties

UV-Vis absorption and photoluminescence (PL) properties of **4a-4c** and **8a-8c** in different solvents investigated are shown in Fig. 6, 7 (in CHCl₃) and 8 (for **4a** and **8a** in different solvents and other data are shown in SI) and the pertinent data are listed in Table 3a and 4. All these compounds have similar structured absorption spectra (Fig. 6a and 6b) with three bands located ranging between 340–400 nm, which were assigned to $\pi\text{-}\pi^*$ transition arising from the characteristic vibrational structures of isolated anthracene moiety.^{51,52,53} Absorption band in the range of 280–300 nm for all compounds could be assigned to the group at the 9-position of the central anthracene core.⁵⁴ Compounds **4a**, **4b**, **8a** and **8b** have similar absorption peak at 290 nm, where as for **4c** and **8c** are ~10 nm bathochromically shifted probably due to strong donating methoxy and trimethoxy substituents, respectively. Similar pattern is observed for all compounds in seven different solvents (Table 3a) which suggests that small dipole moment is associated with these molecules in the ground state.^{55,56}

To have a deeper understanding of the absorption spectra, we have carried out TDDFT calculations, including the solvent effect, in various solvents (Hexane, CHCl₃ and CH₃OH) using PCM model. The results obtained are shown in Table 3b. From these results we observe that there is no noticeable solvatochromic effect for these molecules which is in line with the experimental results (Table 3a). Calculated oscillator strengths (*f*) and corresponding CI of wave function values are also given in the same Table. The major transitions at the orbital level in all the molecules are observed to be HOMO-LUMO, which is localized on the anthracene moiety. The MO picture for **4a** and **8a** of the molecules is shown in Figure 5. The simulated spectra of **4a** and **8a** are presented in SI (Fig.10).

In comparison with absorption spectra, the emission spectra (PL) of certain compounds are sensitive to the polarity of solvents and the fluorescence data generated is arranged in Table 4. PL spectra of compounds **4a-4c** (Fig. 7a in chloroform and for other data see SI) show a broad structure less emission, where as compounds **8a-8c** (Fig. 7b in chloroform and for other data see SI) display structured emission indicating the emission behavior linked with *para* and *meta* substitution. Broad structure less emission is an indication of charge transfer character of the excited state.^{55,57} Photoluminescence recorded for **4a-4c** (Fig. 8a for **4a** and for other compounds see SI) in various solvents exhibited fluorescence solvatochromism, where as compounds **8a-8c** (Fig. 8b for compound **8a** and for other compounds see SI) did not respond to solvent polarity. The fluorescence solvatochromism phenomenon (407–453 nm; Table 4) can be explained by solvent interaction with the excited state and also an indication of polarized nature of the excited state.⁵⁵ Compounds **8a-8c** do not show any solvatochromic effects indicating less dipole interactions with different polar solvents may be because of twisted geometry and may not possess excited state polar character. PL spectra are also recorded in solid state for this series of compounds. Compounds in the solid state exhibited more red shifted (444–513 nm) emission spectra than in dilute solution indicating stronger intermolecular interactions. Fluorescence quantum yields (Φ) were measured in dichloromethane relative to 9,10-diphenylanthracene ($\Phi = 0.9$).⁴⁰ The quantum yields are very good for all the compounds (Table 4). The higher emission yields for **8a-8c** (0.92–0.95), may be due to anthracene and oxadiazole moieties connected through *meta* linkage. There is a decrease of quantum yields for **4a-4c** (0.61–0.68) compared to **8a-8c** because of *para* linkage of anthracene and oxadiazole moieties, which increases the conjugation and planarity.^{38,58} The high quantum yields of these anthracene derivatives make them excellent candidates for use as an efficient light-emitting materials in OLEDs. Optical band gaps obtained from absorption threshold are in the range of 3.08–3.19 eV.

3.6. Electroluminescent properties

Un-optimized OLEDs were fabricated using anthracene derivatives **4a-4c** and **8a-8c** as an emitters with the device configuration: ITO (120 nm)/ α -NPD (30 nm)/**4a-4c** or **8a-8c** (35 nm)/BCP (6 nm)/Alq₃ (28 nm)/LiF (1 nm)/Al (150 nm), where 4,4'-bis[N-(1-naphthyl)-N-phenyl-l-amino]-biphenyl (α -NPD) was used as the hole-transporting layer, BCP was used as hole blocking layer, Alq₃ was used as the electron-transporting layer, LiF and Al were used as the electron injecting layer and cathode, respectively. The corresponding current densities vs. voltage curves were obtained for all fabricated devices (Fig. 9 for **4a** and **8a** and for other compounds see SI). The characteristics of the current density against the applied voltage reveal good diode behavior. The driving voltage for device **4a-4c** is high around 9–12 V, whereas for devices with **8a-8c** show decrease in turn on voltage to about 7 V (Table 5). The ECL emission in **8a-8c** series is slightly blue shifted in comparison to **4a-4c** series due to *meta* linkage (Fig. 10 for **4a** and **8a** and for other compounds see SI), which decreases conjugation. The color of the light achieved is bluish-green in all the cases. The CIE coordinates calculated for the compounds are shown in Table 5. The device characteristic for **8b** is slightly different from its series, ECL emission peaking at 515 and 553 nm. Moreover, its emission is entering into the yellowish-white region of the CIE color space (0.32, 0.42). The devices with each emitter show good stability up to high voltage range. Compared to the fluorescence spectra (Table 4) the ECL spectra are red shifted (Table 5). Among the six anthracene derivatives (**4a-4c** and **8a-8c**) investigated, **8a** displayed highest luminescence of 1728 cd/m² at a current density of 326.7 mA cm⁻² as an emitter. The maximum current efficiency and power efficiency for all devices are shown in Table 5 (Fig. 11 for **4a** and **8a** and for other compounds see SI).

In addition, **8a** was investigated as electron transport layer (ETL) by fabricating two different devices with phosphorescent emitter Ir(ppy)₃ doped 4,4'-bis(9-carbazolyl)-biphenyl (CBP) with the device configuration: ITO (120 nm)/ α -NPD (30 nm)/Ir(ppy)₃ doped CBP (35 nm)/BCP (6 nm)/**8a** or Alq₃ (28 nm)/LiF (1 nm)/Al (150 nm). Only the ETL was changed in the device while the rest of the device was kept same. The first device was with **8a** as an

ETL, while in the second case Alq₃ was used as ETL and the pertinent data is given in Table 6. These results reveal that by using **8a** as an electron transport layer a significant increase in current efficiency at all voltages and almost equivalent luminescence is achieved to the standard Alq₃. Thus it can be summarized that the anthracene derivative **8a** shows superior electron transport property to that of the commercially reported Alq₃.

Further, compound **8a** was tested in bi layer device architecture to know the electron transport emitting character (Table 7). From the performance data generated it is evident that **8a** can act as electron transporting emitter with good current and power efficiency.

4.0 Conclusion

In summary, a series of novel anthracene-oxadiazole based compounds **4a-4c** and **8a-8c** have been designed and synthesized in a facile and easy synthetic strategy, as emitters for non-doped organic light emitting devices. Thermal properties like T_d (297–364 °C), T_m (204–236 °C) and T_g (82–98 °C) were evaluated, which indicate good stability of the compounds. Electrochemical properties like HOMO, LUMO energy values determined using cyclic voltammetry (CV), are in correlation with the data generated by computational analysis (TD-DFT). The compounds studied have reversible oxidation and quasi reversible reductions and those values indicate that the compounds could be suitable for electron transporting as well as hole blocking material for electroluminescent devices. The study of photo physical properties in different solvents as well as in solid state reveal blue emission originating from electronic $\pi-\pi^*$ excited states. The fluorescence solvatochromism observed in **4a-4c** indicate the polar nature in excited state. The absorption maxima determined experimentally are in concurrence with the values determined by TD-DFT calculations. The fluorescence quantum yields measured are found to be excellent for **8a-8c** and good for **4a-4c**. In an un-optimized, non-doped OLED device configuration, **8a** displayed high brightness 1728 cd m⁻² and a current efficiency of 0.89 cd A⁻¹ compared to other compounds. Electron transport property evaluated for **8a** shows current efficiency of 11.7 cd A⁻¹ (compared to the standard electron transport material Alq₃, 8.69 cd A⁻¹) demonstrating its potential use in OLED.

Current results demonstrate that the anthracene-oxadiazole based compounds are promising electron-transport material for the fabrication of OLEDs. Further, these molecules can serve as basis in designing better performing small molecules for non-doped OLEDs.

Acknowledgements

The authors GM, MAR thank UGC and SB thank CSIR for fellowships. We thank the Director, CSIR-IICT for encouragement. We acknowledge NWP-0055 project for funding.

References

- 1) C.W. Tang and S. A. VanSlyke, Organic electroluminescent diodes, *Appl. Phys. Lett.*, 1987, **51**, 913–915.
- 2) J. H. Burroughes, D. D. C. Bradley, A. R. Broun, R. N. Marks, K. Mackay, R. H. Friend, P. L. Burn and A. B. Holmes, Light-emitting diodes based on conjugated polymers, *Nature*, 1990, **347**, 539–541.
- 3) M. Zhu and C. Yang, Blue fluorescent emitters: design tactics and applications in organic light-emitting diodes, *Chem. Soc. Rev.*, 2013, **42**, 4963–4976.
- 4) S. Yoo, H. Yun, Kang, K. Thangaraju, S. Kwon and Y. Kim, A new electron transporting material for effective hole-blocking and improved charge balance in highly efficient phosphorescent organic light emitting diodes, *J. Mater. Chem. C*, 2013, **1**, 2217–2223.
- 5) O. Nuyken, S. Jungermann, V. Wiederhorn, E. Bacher and K. Meerholz, Modern Trends in Organic Light-Emitting Devices (OLEDs), *Monatsh. Chem.* 2006, **137**, 811–824.
- 6) Y. H. Kim, S. J. Lee, S. Y. Jung, K. N. Byeon, J. S. Kim, S. C. Shin and S. K. Kwon, Synthesis and Characterization of Novel Red-Light-Emitting Materials with Push-Pull

- Structure Based on Benzo[1,2,5]thiadiazole Containing Arylamine as an Electron Donor and Cyanide as an Electron Acceptor, *Bull. Korean Chem. Soc.*, 2007, **28**, 443–446.
- 7) R. M. Adhikari, R. Mondal, B. K. Shah and D. C. Neckers, Synthesis and Photophysical Properties of Carbazole-Based Blue Light-Emitting Dendrimers, *J. Org. Chem.*, 2007, **72**, 4727–4732.
- 8) X. Xu, G. Yu, S. Chen, C. Di and Y. Liu, Synthesis and characterization of a quinoxaline compound containing polyphenylphenyl and strong electron-accepting groups, and its multiple applications in electroluminescent devices, *J. Mater. Chem.*, 2008, **18**, 299–305.
- 9) Q. Tong, S. Lai, M. Chan, Y. Zhou, H. Kwong, C. Lee and S. Lee, Highly Efficient Blue Organic Light-Emitting Device Based on a Nondoped Electroluminescent Material, *Chem. Mater.* 2008, **20**, 6310–6312.
- 10) M. A. Reddy, G. Mallesham, K. Bhanuprakash and V. J. Rao, Organic Light Emitting Devices (OLEDs): Working Principle, *SMC Bulletin*, 2012, **3**, 1–12.
- 11) V. J. Rao, G. Mallesham, G. S. Kumar and B. A. Rao, Recent Advances in Materials for Organic Light Emitting Devices, *Research signpost publications* (book under release), ISBN 978-81-308-0508-5.
- 12) Z. Li and H. Meng, Organic Light-Emitting Materials and Devices, Taylor and Francis Group, LLC, Boca Raton, 2007.
- 13) W. Hung, T. Tsai, S. Ku, L. Chi and K. Wong, An ambipolar host material provides highly efficient saturated red PhOLEDs possessing simple device structures, *Phys. Chem. Chem. Phys.*, 2008, **10**, 5822–5825.
- 14) M. T. Lee, H. H. Chen, C. H. Liao, C. H. Tsai and C. H. Chen, Stable styrylamine-doped blue organic electroluminescent device based on 2-methyl-9,10-di(2-naphthyl)anthracene, *Appl. Phys. Lett.* 2004, **85**, 3301–3303.
- 15) C. W. Tang, S. A. VanSlyke and C. H. Chen, Electroluminescence of doped organic thin films, *J. Appl. Phys.*, 1989, **65**, 3610.

- 16) N. J. Turro, *Modern Molecular Photochemistry*, Benjamin Cumming, Menlo park, CA, 1978, 191.
- 17) M. A. Baldo, C. Adachi and S. R. Forrest, Transient analysis of organic electrophosphorescence. II. Transient analysis of triplet-triplet annihilation, *Phys. Rev. B: Condens. Matter*, 2000, **62**, 10967-10977.
- 18) C. Wang, L.O. Palsson, A.S. Batsanov and M.R. Bryce, Molecular Wires Comprising π -Extended Ethynyl- and Butadiynyl-2,5-Diphenyl-1,3,4-Oxadiazole Derivatives: \square Synthesis, Redox, Structural, and Optoelectronic Properties, *J. Am. Chem. Soc.* 2006, **128**, 3789 \square 3799.
- 19) J. You, S. Lai, W. Liu, T. Ng, P. Wang and C. Lee, Bipolar cyano-substituted pyridine derivatives for applications in organic light-emitting devices, *J. Mater. Chem.*, 2012, **22**, 8922–8929.
- 20) Y. Chi and P. T. Chou, Transition-metal phosphors with cyclometalating ligands: fundamentals and applications, *Chem. Soc. Rev.*, 2010, **39**, 638–655.
- 21) S. R. Forrest, The path to ubiquitous and low-cost organic electronic appliances on plastic, *Nature*, 2004, **428**, 911 \square 918.
- 22) C. Adachi, M. A. Baldo, S. R. Forrest and M. E. Thompson, High-efficiency organic electrophosphorescent devices with tris[2-Phenylpyridine] iridium doped into electron-transporting materials, *Appl. Phys. Lett.*, 2000, **77**, 904 \square 906.
- 23) U. Muller, M. Adam, and K. Miillen, Synthesis and Characterization of Soluble Oligo(9,10-anthrylene), *Chem. Ber.* 1994, **127**, 437 \square 444.
- 24) A. Dadvand, W. H. Sun, A. G. Moiseev, F. B. Gariepy, F. Rosei, H. Meng and D. F. Perepichka, 1,5-, 2,6- and 9,10-distyrylanthracenes as luminescent organic semiconductors, *J. Mater. Chem. C*, 2013, **1**, 2817 \square 2825.
- 25) J. Jou, Y. Chen, J. Tseng, R. Wu, J. Shyue, K. R. J. Thomas, N. Kapoor, C. Chen, Y. Lin, P. Wang, H. Hung, J. Li, and S. Chen, The use of a polarity matching and high-energy exciton generating host in fabricating efficient purplish-blue OLEDs from a sky-blue emitter, *J. Mater. Chem.*, 2012, **22**, 15500 \square 15506.

- 26) T. M. F. Duarte and K. Mullen, Pyrene-Based Materials for Organic Electronics, *chemical review*, 2011, **111**, 7260–7314.
- 27) O. Usluer, S. Demic, D. A. M. Egbe, E. Birckner, C. Tozlu, A. Pivrikas, A. M. Ramil, and N. S. Sariciftci, Fluorene-Carbazole Dendrimers: Synthesis, Thermal, Photophysical and Electroluminescent Device Properties, *Adv. Funct. Mater.* 2010, **20**, 4152–4161.
- 28) C. Chiang, M. Wu, D. Dai, Y. Wen, J. Wang, and C. Chen, Red-Emitting Fluorenes as Efficient Emitting Hosts for non-Doped, Organic Red-Light-Emitting Diodes, *Adv. Funct. Mater.* 2005, **15**, 231–238.
- 29) Z. Li, B. Jiao, Z. Wu, P. Liu, L. Ma, X. Lei, D. Wang, G. Zhou, H. Hud and X. Hou, Fluorinated 9,9'-spirobifluorene derivatives as host materials for highly efficient blue organic light-emitting devices, *J. Mater. Chem. C*, 2013, **1**, 2183–2192.
- 30) N. Kapoor and K. R. J. Thomas, Fluoranthene-based triarylaminines as hole-transporting and emitting materials for efficient electroluminescent devices, *New J. Chem.*, 2010, **34**, 2739–2748.
- 31) Y. Tao, Q. Wang, Y. Shang, C. Yang, L. Ao, J. Qin, D. Ma and Z. Shuai, Multifunctional bipolar triphenylamine/oxadiazole derivatives: highly efficient blue fluorescence, red phosphorescence host and two-color based white OLEDs, *Chem. Commun.*, 2009, 77–79.
- 32) S. Kim, I. Cho, M. Sim, S. Park and S. Y. Park, Highly efficient deep-blue emitting organic light emitting diode based on the multifunctional fluorescent molecule comprising covalently bonded carbazole and anthracene moieties, *J. Mater. Chem.*, 2011, **21**, 9139–9148.
- 33) M. Ren, H. Guo, F. Qi and Q. Song, Fluorescent pyrene-centered starburst oligocarbazoles with excellent thermal and electrochemical stabilities, *Org. Biomol. Chem.*, 2011, **9**, 6913–6916.
- 34) S. Zhang, R. Chen, J. Yin, F. Liu, H. Jiang, N. Shi, Z. An, C. Ma, B. Liu, and W. Huang, Tuning the Optoelectronic Properties of 4,4'-N,N'-Dicarbazole-biphenyl through

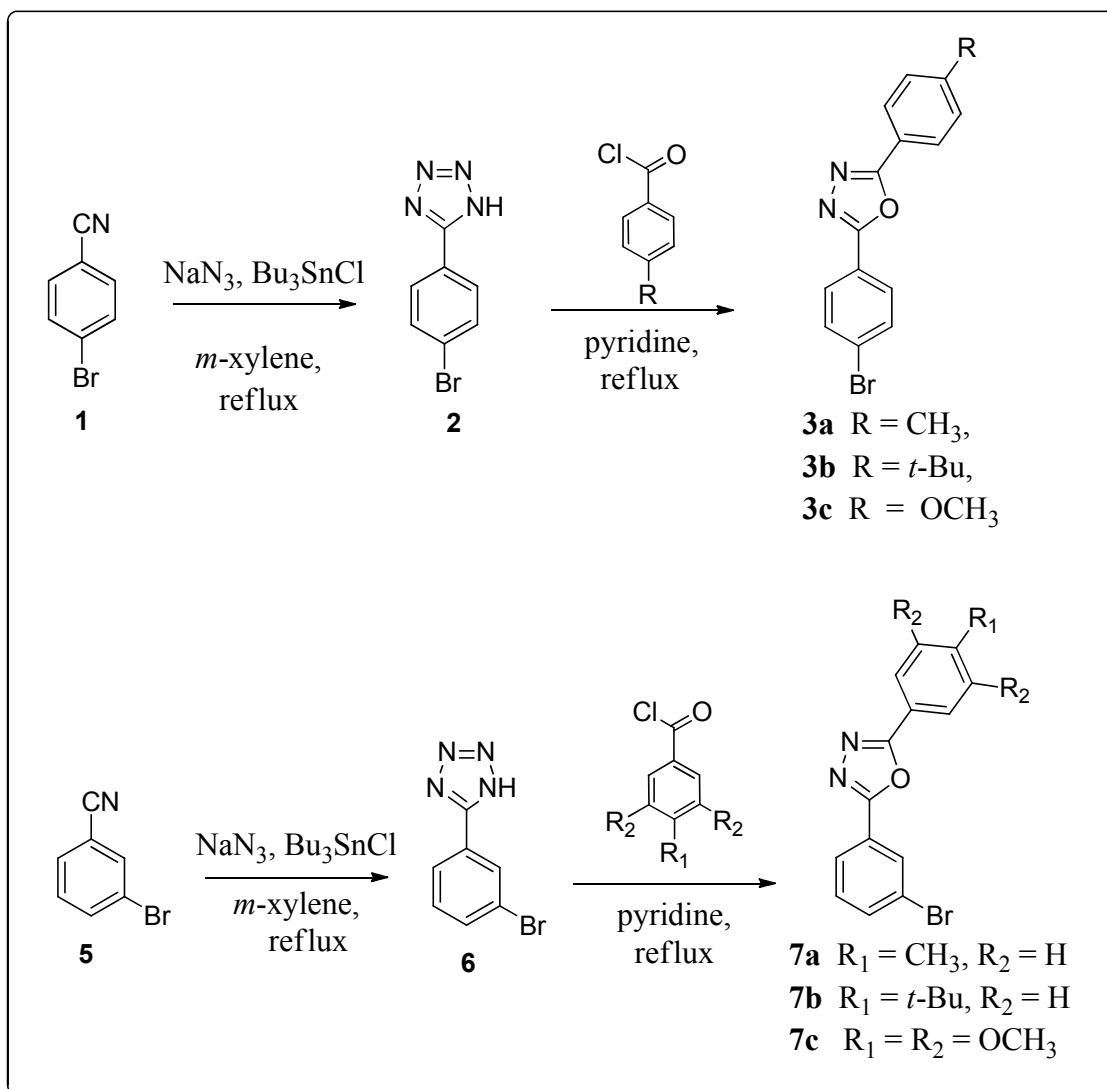
- Heteroatom Linkage: New Host Materials for Phosphorescent Organic Light-Emitting Diodes, *Org. Lett.*, 2010, **12**, 3438–3441.
- 35) Y. Chen, H. Chou, T. Su, P. Chou, F. Wu and C. Cheng, Synthesis and photo- and electroluminescence properties of 3,6-disubstituted phenanthrenes: alternative host material for blue fluorophores, *Chem. Commun.*, 2011, **47**, 8865–8867.
- 36) S. Lin, F. Wu and R. Liu, Synthesis, photophysical properties and color tuning of highly fluorescent 9,10-disubstituted-2,3,6,7-tetraphenylanthracene, *Chem. Commun.*, 2009, 6961–6963.
- 37) M. A. Reddy, A. Thomas, K. Srinivas, V. J. Rao, K. Bhanuprakash, B. Sridhar, A. Kumar, M. N. Kamalasanan and R. Srivastava, Synthesis and characterization of 9,10-bis(2-phenyl-1,3,4-oxadiazole) derivatives of anthracene: Efficient n-type emitter for organic light-emitting diodes, *J. Mater. Chem.*, 2009, **19**, 6172–6184.
- 38) M. A. Reddy, G. Mallesham, A. Thomas, K. Srinivas, V. J. Rao, K. Bhanuprakash, L. Giribabu, R. Grover, A. Kumar, M. N. Kamalasanan and R. Srivastava, Synthesis and characterization of novel 2,5-diphenyl-1,3,4-oxadiazole derivatives of anthracene and its application as electron transporting blue emitters in OLEDs, *Synthetic Metals*, 2011, **161**, 869–880.
- 39) M. A. Reddy, A. Thomas, G. Mallesham, B. Sridhar, V. J. Rao and K. Bhanuprakash, Synthesis of novel twisted carbazole–quinoxaline derivatives with 1,3,5-benzene core: bipolar molecules as hosts for phosphorescent OLEDs, *Tetrahedron Letters*, 2011, **52**, 6942–6947.
- 40) S. R. Meech and D. Phillips, Photophysics of some common fluorescence standards, *J. Photochem.*, 1983, **23**, 193–217.
- 41) H. S. Wang, M. S. Su, and K. H. Wei, Synthesis and Characterization of Donor–Acceptor Poly(3-hexylthiophene) Copolymers Presenting 1,3,4-Oxadiazole Units and Their Application to Photovoltaic Cells, *J. Polym. Sci. Part A. Polym. Chem.*, 2010, **48**, 3331–3339.

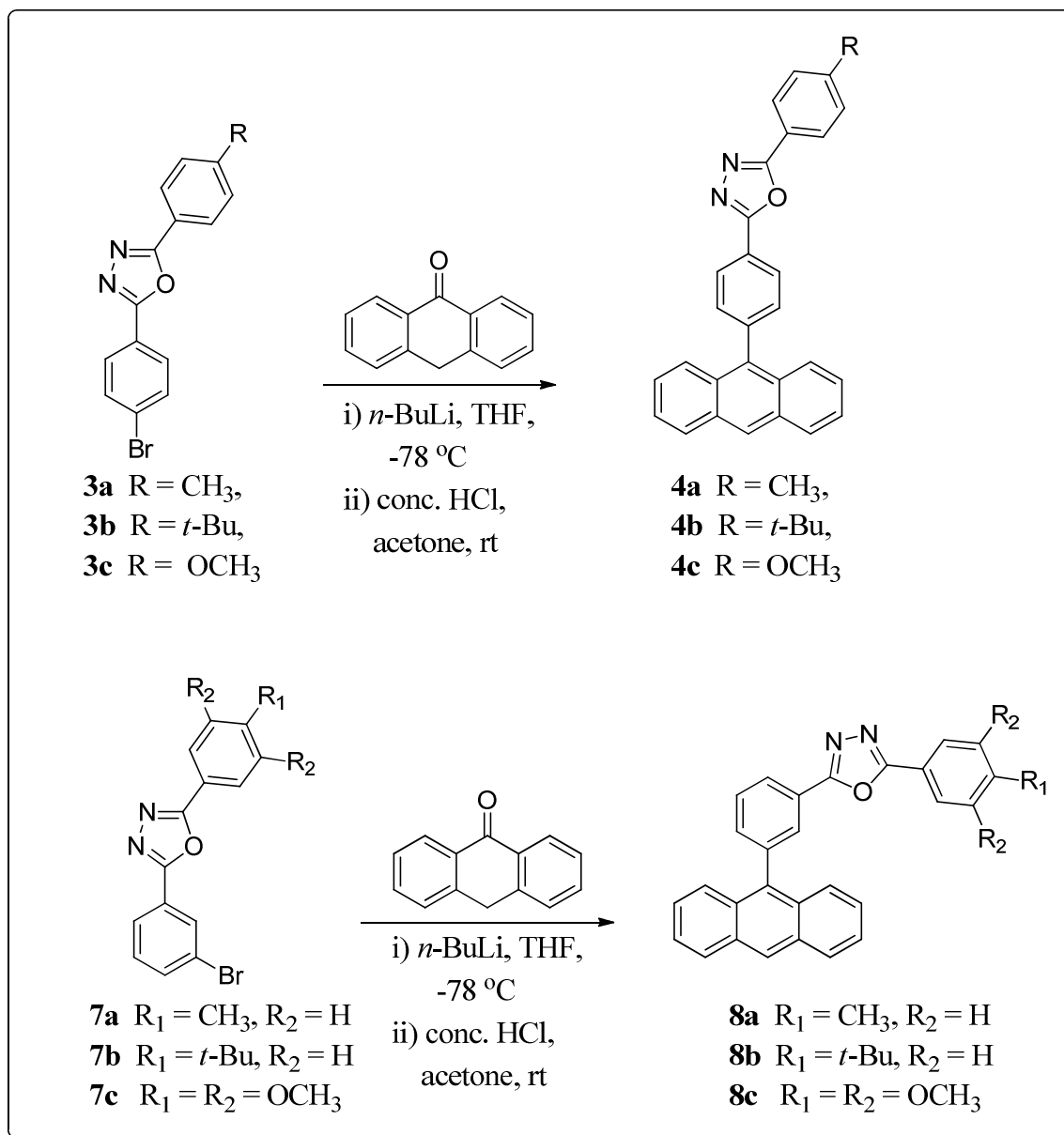
- 42) H. Y. Chen, C. T. Chen and C. T. Chen, Synthesis and Characterization of a New Series of Blue Fluorescent 2,6-Linked 9,10-Diphenylanthrylenephenylene Copolymers and Their Application for Polymer Light-Emitting Diodes, *Macromolecules*, 2010, **43**, 3613-3623.
- 43) H. Wang, J. Ryu, Y. H. Shin and Y. Kwon, Synthesis and Properties of Polymers Containing Charge Transport Pendant Group, *Mol. Cryst. Liq. Cryst.*, 2009, **514**, 158-170.
- 44) Z. Shang, Oxidative Cyclization of Aromatic Aldehyde N-Acylhydrazones by bis(Trifluoroacetoxy)iodobenzene, *Synthetic Communications*, 2006, **36**, 2927-2937.
- 45) G. Scalmani and M. J. Frisch, Continuous surface charge polarizable continuum models of solvation. I. General formalism, *J. Chem. Phys.*, 2010, **132**, 114110-114115.
- 46) *Gaussian 09*, Revision B.01, M. J. Frisch, G. W. Trucks, H. B. Schlegel, G. E. Scuseria, M. A. Robb, J. R. Cheeseman, G. Scalmani, V. Barone, B. Mennucci, G. A. Petersson, H. Nakatsuji, M. Caricato, X. Li, H. P. Hratchian, A. F. Izmaylov, J. Bloino, G. Zheng, J. L. Sonnenberg, M. Hada, M. Ehara, K. Toyota, R. Fukuda, J. Hasegawa, M. Ishida, T. Nakajima, Y. Honda, O. Kitao, H. Nakai, T. Vreven, Jr. J. A. Montgomery, J. E. Peralta, F. Ogliaro, M. Bearpark, J. J. Heyd, E. Brothers, K. N. Kudin, V. N. Staroverov, R. Kobayashi, J. Normand, K. Raghavachari, A. Rendell, J. C. Burant, S. S. Iyengar, J. Tomasi, M. Cossi, N. Rega, N. J. Millam, M. Klene, J. E. Knox, J. B. Cross, V. Bakken, C. Adamo, J. Jaramillo, R. Gomperts, R. E. Stratmann, O. Yazyev, A. J. Austin, R. Cammi, C. Pomelli, J. W. Ochterski, R. L. Martin, K. Morokuma, V. G. Zakrzewski, G. A. Voth, P. Salvador, J. J. Dannenberg, S. Dapprich, A. D. Daniels, O. Farkas, J. B. Foresman, J. V. Ortiz, J. Cioslowski, D. J. Fox, Gaussian, Inc., Wallingford CT, 2010.
- 47) A. V. Dijken, J. J. A. M. Bastiaansen, N. M. M. Kiggen, B. M. W. Langeveld, C. Rothe, A. Monkman, I. Bach, P. Stossel and K. Brunner, Carbazole Compounds as Host Materials for Triplet Emitters in Organic Light-Emitting Diodes: Polymer Hosts for High-Efficiency Light-Emitting Diodes, *J. Am. Chem. Soc.*, 2004, **126**, 7718-7727.

- 48) C. Du, S. Ye, Y. Liu, Y. Guo, T. Wu, H. Liu, J. Zheng, C. Cheng, M. Zhu and G. Yu, Fused-seven-ring anthracene derivative with two sulfur bridges for high performance red organic light-emitting diodes, *Chem. Commun.*, 2010, **46**, 8573–8575.
- 49) S. Janietza, D. D. C. Bradley, M. Grell, C. Giebeler, M. Inbasekaran and E. P. Woo, Electrochemical determination of the ionization potential and electron affinity of poly(9,9-dioctylfluorene), *Appl. Phys. Lett.*, 1998, **73**, 2453–2455.
- 50) A. K. Agrawal and S. A. Jenekhe, Electrochemical Properties and Electronic Structures of Conjugated Polyquinolines and Polyanthrazolines, *Chem. Mater.*, 1996, **8**, 579–589.
- 51) M. J. R. Reddy, V. V. Reddy, U. Srinivas, M. J. R. Reddy, and V. J. Rao, Regioselective *E(trans)*–*Z(trans)* photoisomerization in naphthylidene derivatives, *Proc. Indian Acad. Sci. (Chem. Sci.)*, 2002, **114**, 603–609.
- 52) I. B. Berlman, *Hand Book of Fluorescence Spectra of Aromatic Molecules*, 2nd edn, Academic Press, New York, 1971.
- 53) R. Kim, S. Lee, K. Kim, Y. Lee, S. Kwon, J. Kim and Y. Kim, Extremely deep blue and highly efficient non-doped organic light emitting diodes using an asymmetric anthracene derivative with a xylene unit, *Chem. Commun.*, 2013, **49**, 4664–4666.
- 54) Z. Wang, C. Xu, W. Wang, L. Duan, Z. Li, B. Zhao and B. Ji, High-color-purity and high-efficiency non-doped deep-blue electroluminescent devices based on novel anthracene derivatives, *New J. Chem.*, 2012, **36**, 662–667.
- 55) V. R. Gopal, A. M. Reddy, and V. J. Rao, Wavelength Dependent Trans to Cis and Quantum Chain Isomerization of Anthrylethylene Derivatives, *J. Org. Chem.*, 1995, **60**, 7966–7973.
- 56) V. R. Gopal, V. J. Rao, G. Saroja and A. Samanta, Photophysical behaviour of some pyrenylethylene derivatives and its implication on trans to cis photoisomerisation reactions, *Chemical Physics Letters*, 1997, **270**, 593–598.
- 57) U. Srinivas, P. A. Kumar, K. Srinivas, K. and V. J. Rao, Conformational analysis of 2-anthryl-ethylene derivatives: Photochemical and computational investigation, *Journal of Structural Chemistry*, 2012, **53**, 851–865.

- 58) N. Prachumrak, S. Namuangruk, T. Keawin, S. Jungsuttingwong, T. Sudyoadsuk, and V. Promarak, Synthesis and Characterization of 9-(Fluoren-2-yl)anthracene Derivatives as Efficient Non-Doped Blue Emitters for Organic Light-Emitting Diodes, *Eur. J. Org. Chem.* 2013, 3825–3834.

Figures and Tables:

**Scheme 1:** Reaction scheme for the synthesis of the key intermediates.



Scheme 2. Reaction scheme for the synthesis of the target compounds **4a-4c** and **8a-8c**.

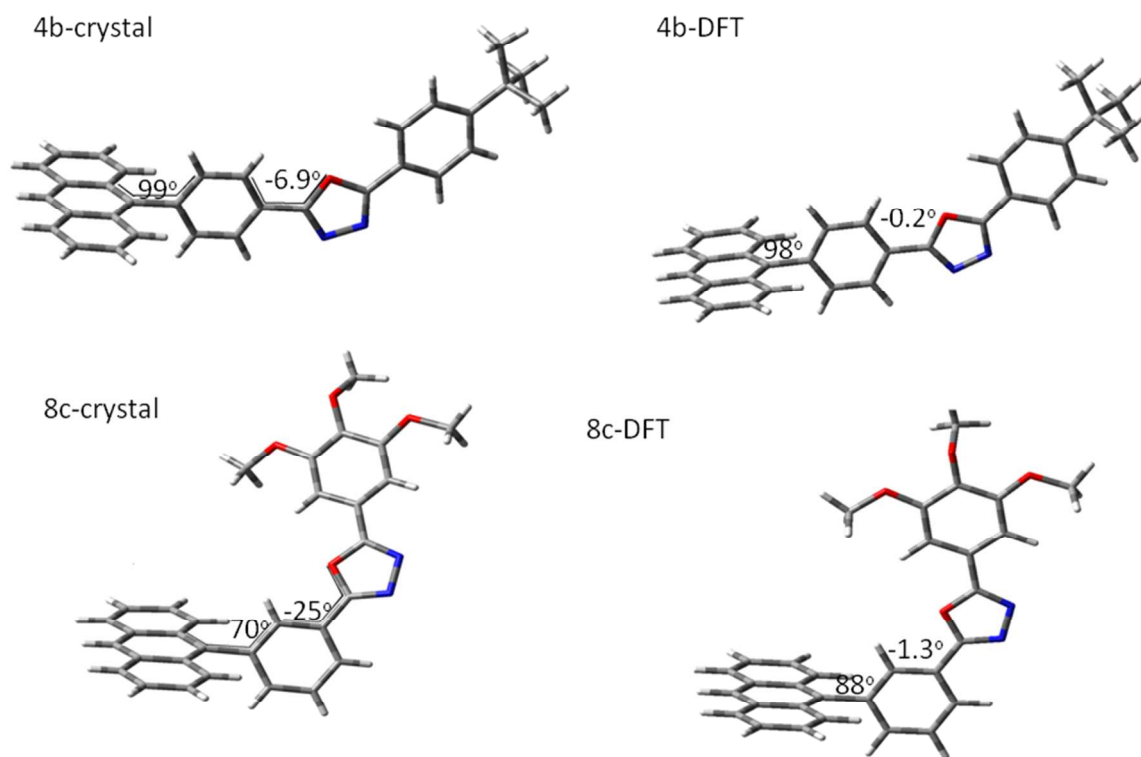
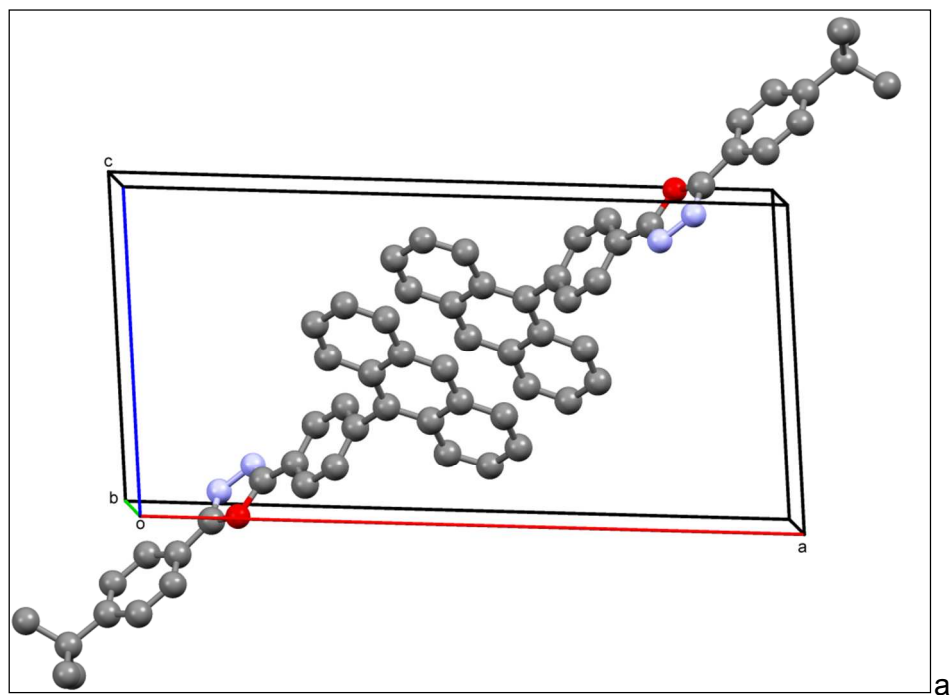


Fig. 1 X-ray molecular structures and B3LYP/6-311G(d,p) optimized molecular structures of **4b** and **8c**

A)



B)

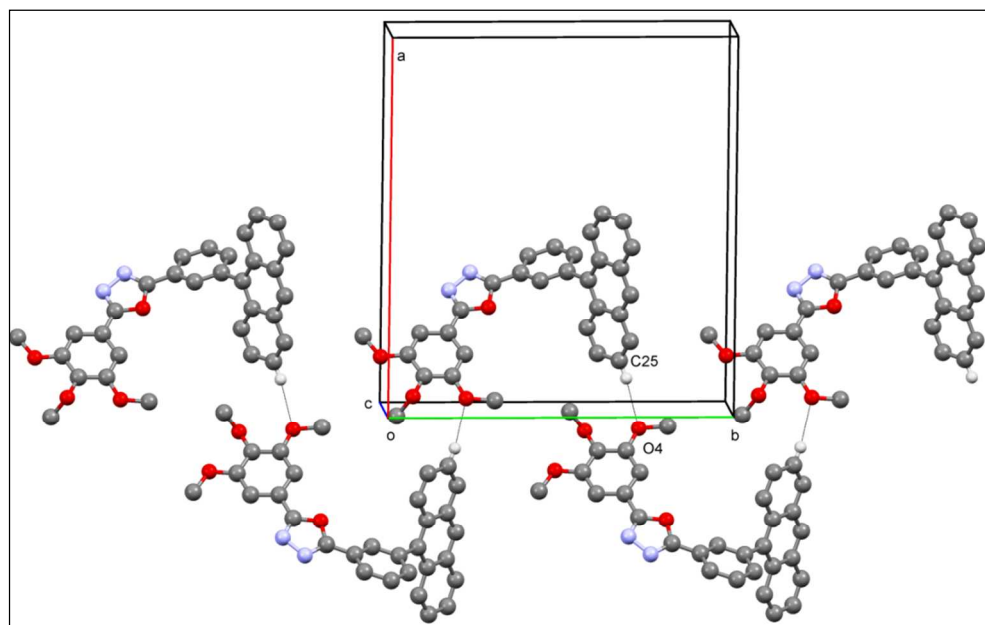


Fig. 2 A. Partial packing diagram for **4b** viewed down the b-axis showing the intermolecular stacking of the anthracene moiety. H atoms have been omitted for clarity. **B.** Partial packing

diagram for **8c** viewed down the c-axis showing the infinite helical chain formed by the CH \cdots O interactions. H atoms not involved in hydrogen bonds have been omitted for clarity.

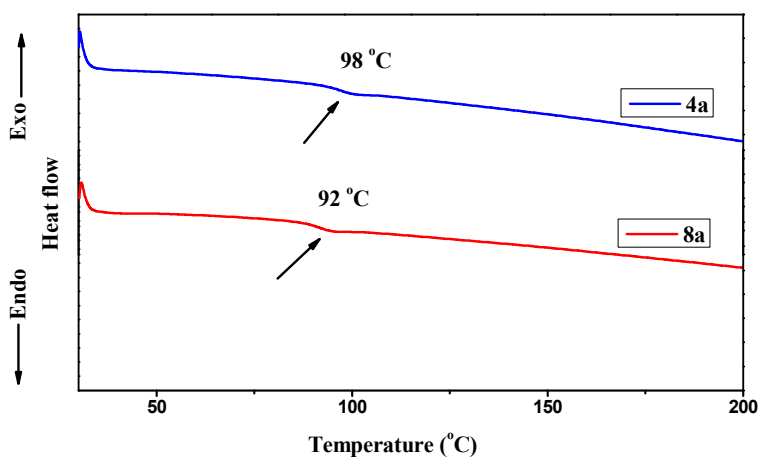
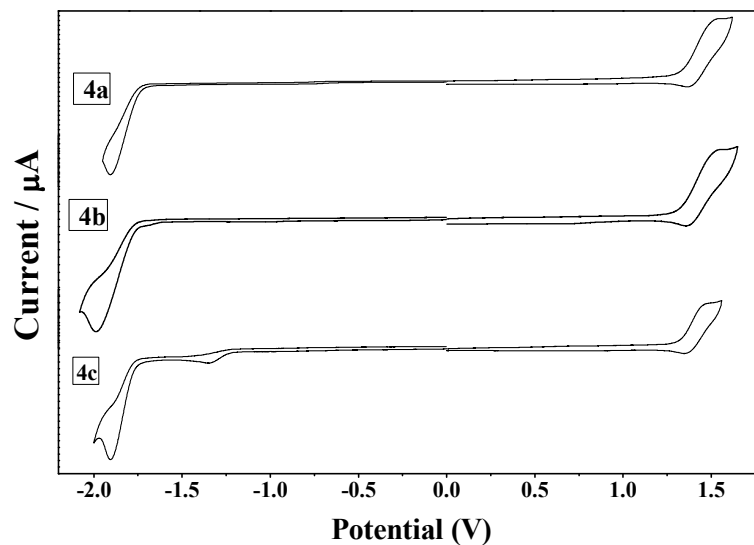


Fig. 3 DSC traces of **4a** and **8a** recorded at a heating rate of 10 °C min⁻¹(for the other compounds please see SI

a)



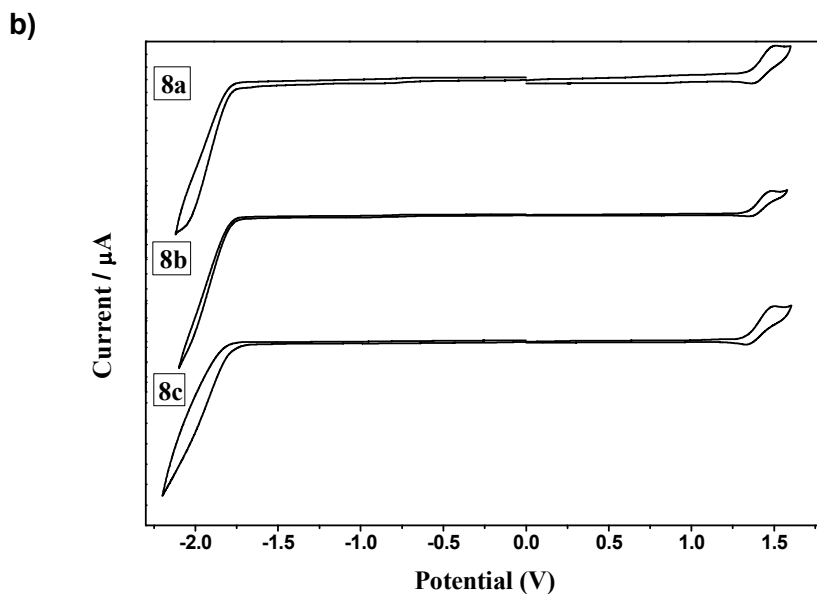


Fig. 4 Cyclic voltammogram of **4a-4c** and **8a-8c** obtained in 0.1 M NBu_4ClO_4 CH_2Cl_2 solution at a scan rate of 100 mVs^{-1} .

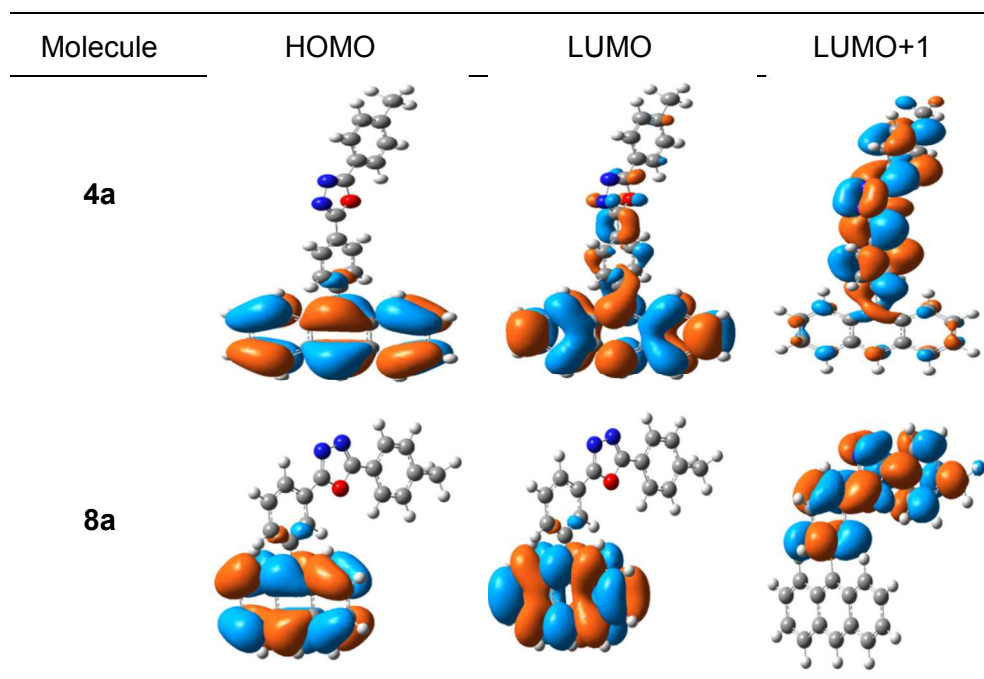


Fig. 5 Frontier molecular orbitals of **4a** and **8a** obtained at B3LYP/6-311G(d,p) level of theory (for the other compounds see SI)

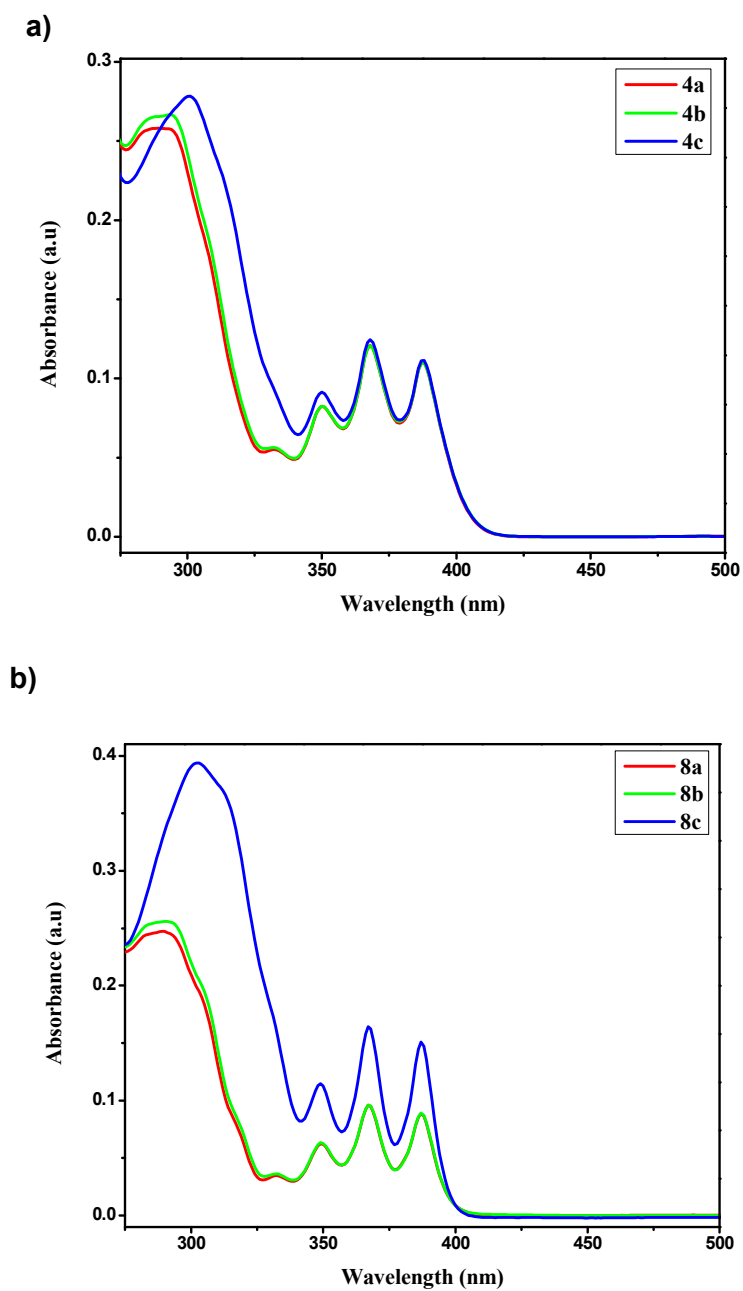


Fig. 6 UV-Vis absorption spectra of compounds **4a-4c** (a) and **8a-8c** (b) in CHCl_3 ($1 \times 10^{-5} \text{ M}$).

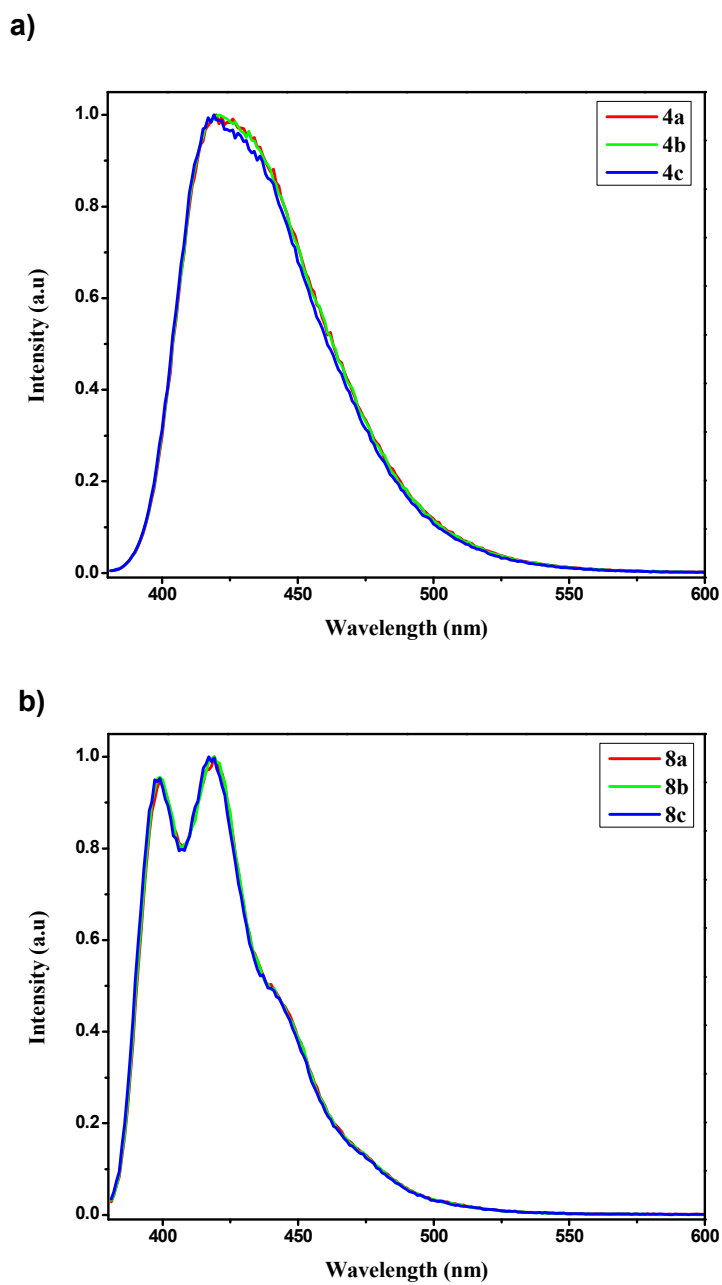


Fig. 7 Normalized PL spectra of compounds **4a-4c** (a) and **8a-8c** (b) in CHCl_3 (1×10^{-5} M).

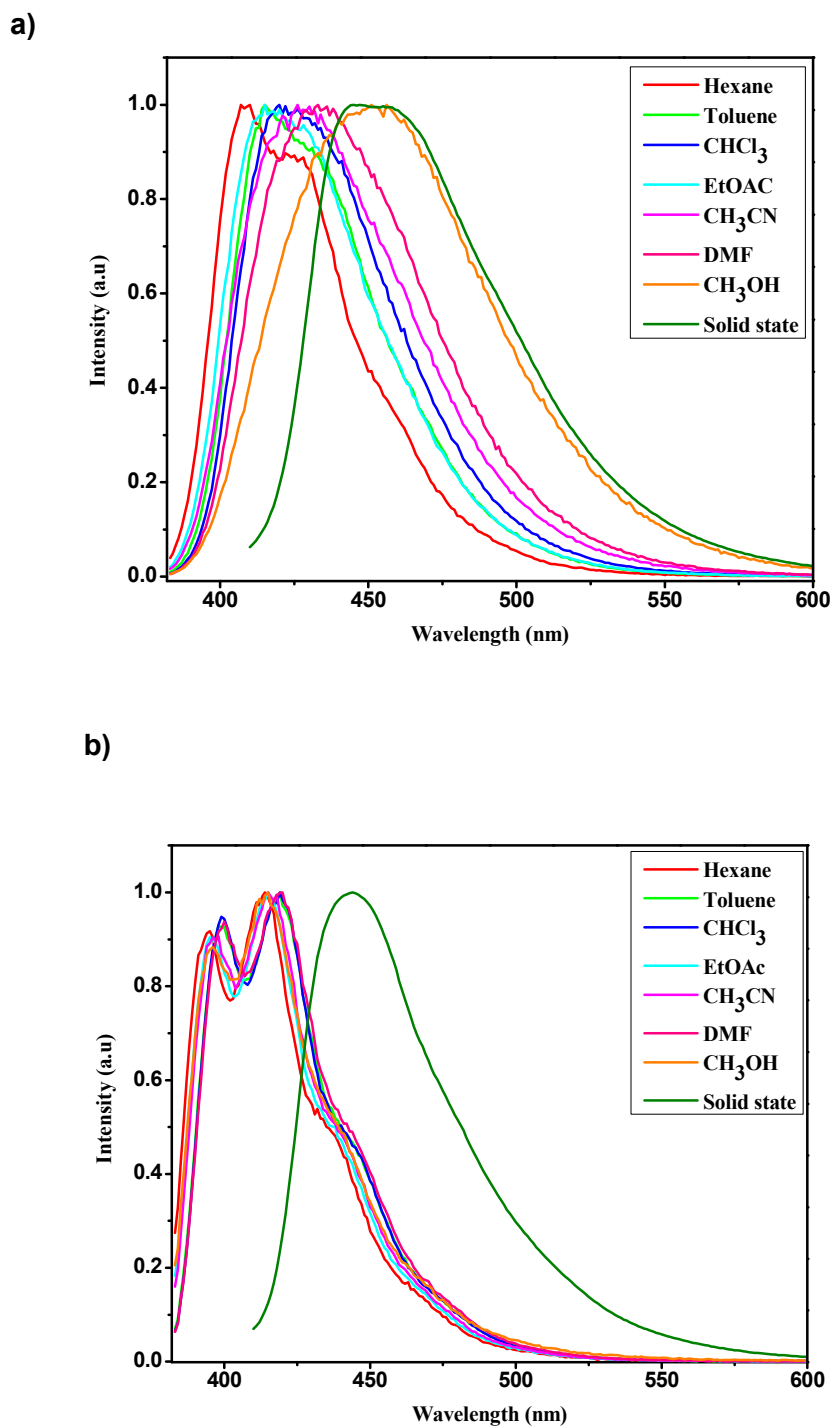


Fig. 8 Normalized emission spectra of **4a** (a) and **8a** (b) in different solvents (1×10^{-5} M) and in solid state carried out at ambient temperature (for the other compounds see SI).

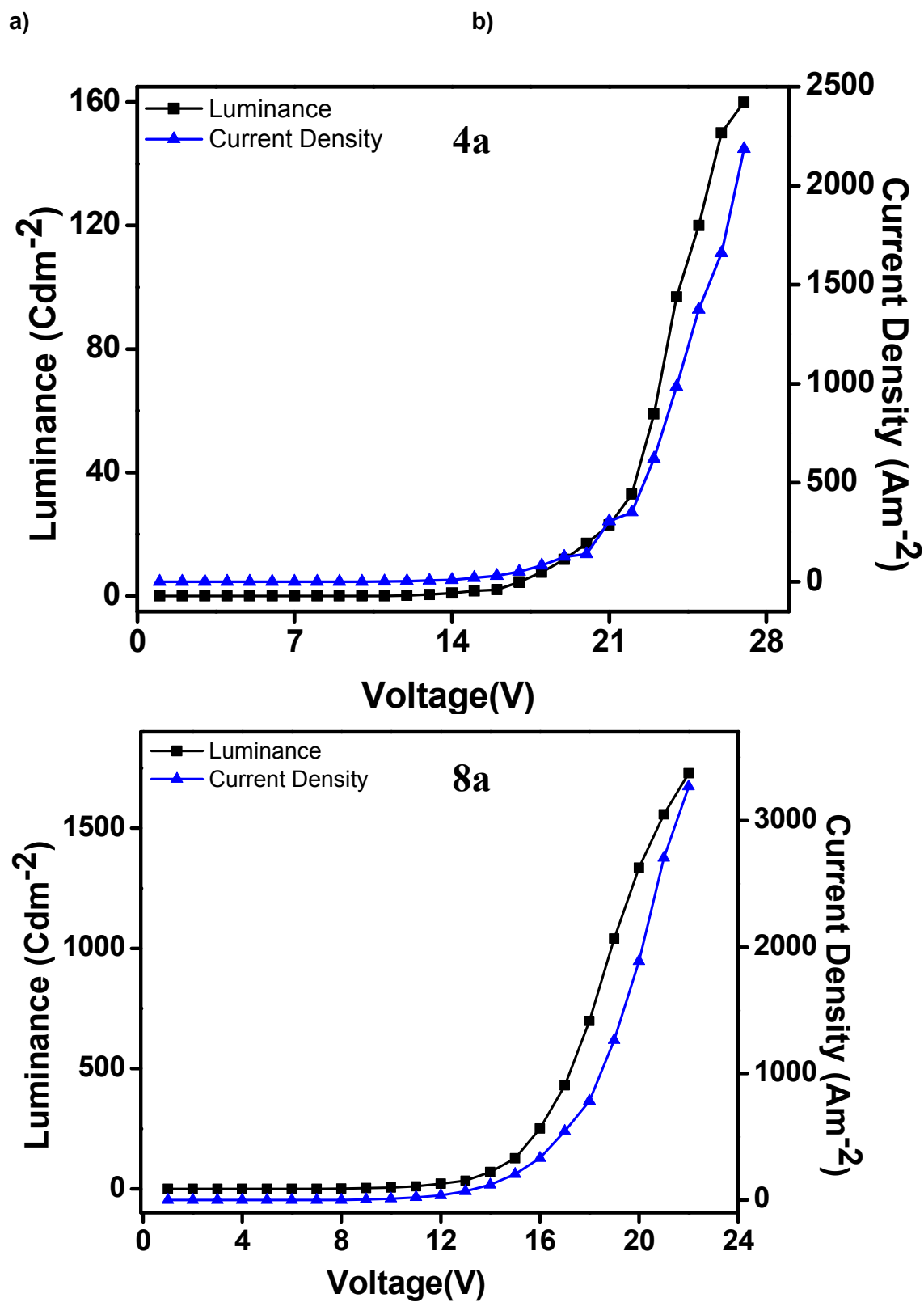


Fig. 9 Current density and luminance curve for 4a (a) and 8a (b) (for the other compounds

see SI).

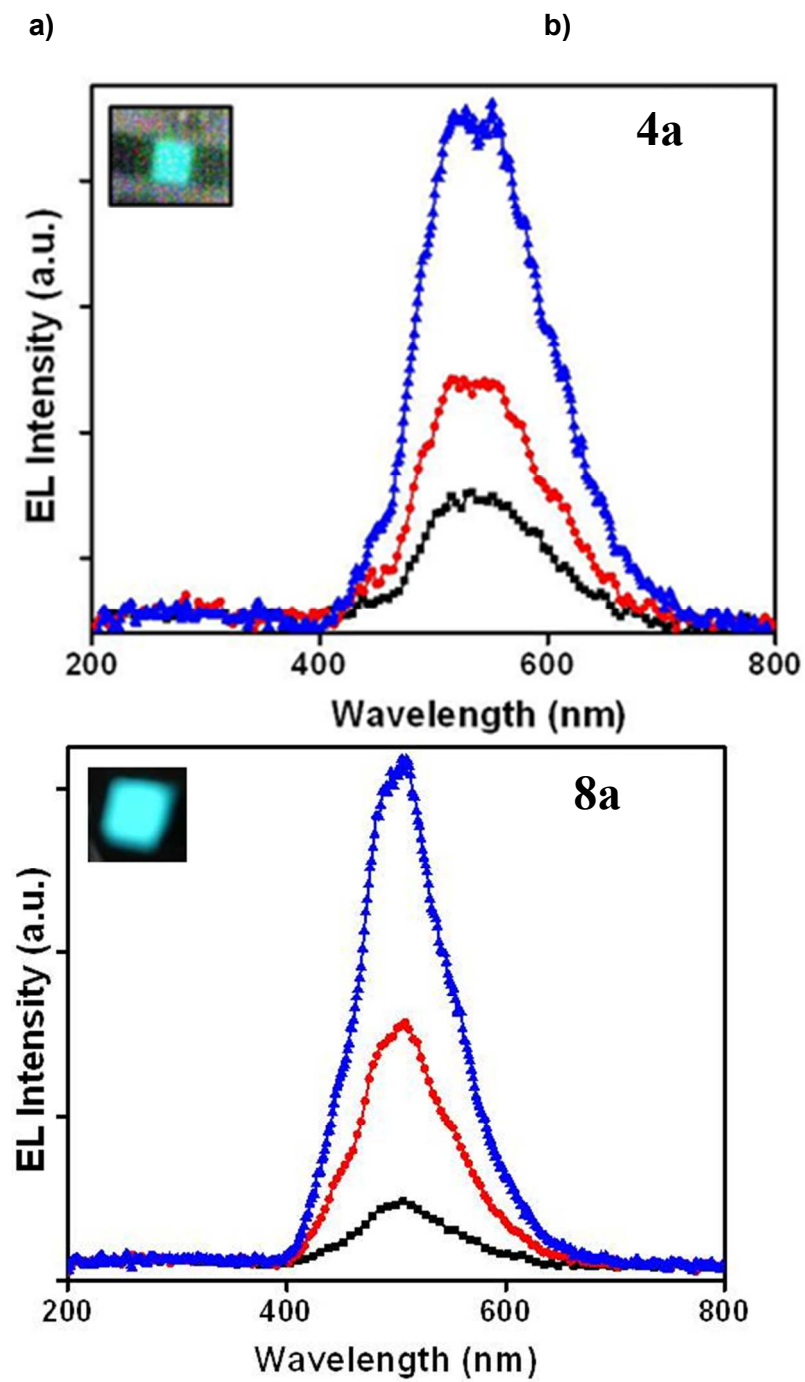


Fig. 10 The characteristic ECL performance data for **4a** (a) and **8a** (b) at 10, 12, 14V (for other compounds see SI)

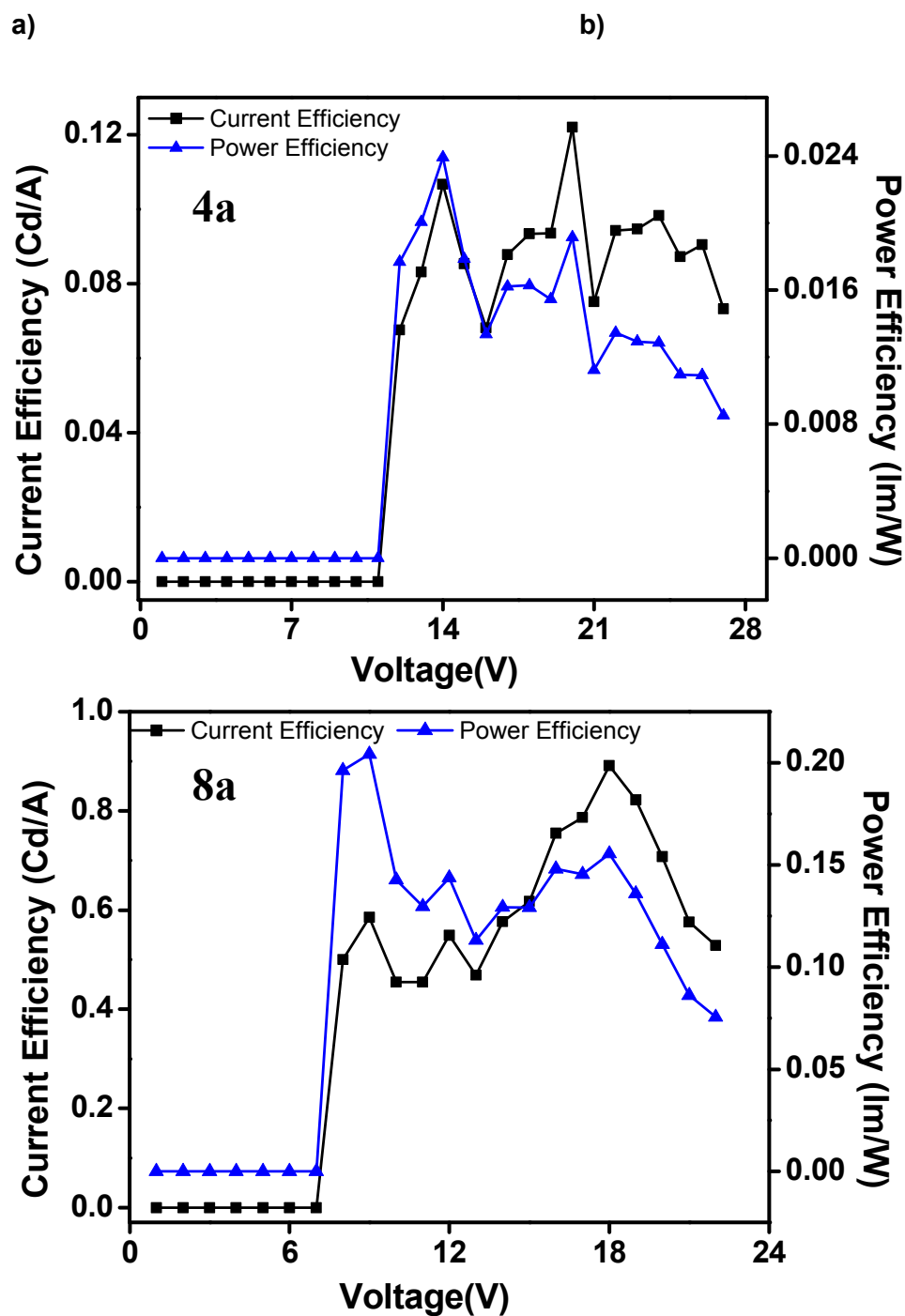


Fig. 11 Current and power efficiency curves for **4a** (a) and **8a** (b) (for other compounds please see SI).

Table 1. Thermal analysis data of **4a-4c** and **8a-8c** obtained from TGA and DSC.

compound	T _d ^a (°C)	T _m ^b (°C)	T _g ^c (°C)
4a	320	210	98
4b	364	236	98
4c	297	220	82
8a	342	204	92
8b	344	207	93
8c	319	232	88

^a T_d: decomposition temperature (corresponding to 5% weight loss). ^b T_m: melting point.

^c T_g: glass transition temperature.

Table 2. Electrochemical data obtained from cyclic voltammetry measurements along with DFT obtained values for comparison.

Compound ^a	E _{ox} ^{onset} ^b (V)	E _{red} ^{onset} ^c (V)	HOMO ^d (eV)	LUMO ^e (eV)	ΔE _{ele} ^f (eV)	HOMO / LUMO / ΔE ^g (eV)	ΔE _{opt} ^h (eV)
4a	1.34	-1.74	-5.74	-2.66	3.08	-5.62 / -2.14 / 3.48	3.11(399)
4b	1.35	-1.75	-5.75	-2.65	3.10	-5.62 / -2.13 / 3.49	3.11(399)
4c	1.34	-1.77	-5.74	-2.63	3.11	-5.60 / -2.11 / 3.48	3.11(400)
8a	1.32	-1.80	-5.72	-2.60	3.12	-5.64 / -2.13 / 3.51	3.17(391)
8b	1.37	-1.81	-5.77	-2.59	3.18	-5.64 / -2.14 / 3.51	3.16(392)

8c	1.35	-1.80	-5.75	-2.60	3.15	-5.63 / -2.12 / 3.51	3.17(391)
-----------	------	-------	-------	-------	------	----------------------	-----------

^a Cyclic voltammetric measurements were performed in 1 mM dichloromethane solution with 0.1M of Bu₄NClO₄ as a supporting electrolyte. ^b Onset potential of oxidation. ^c Onset potential of reduction; ^d HOMO = - (4.4 + E_{ox}^{onset}) eV. ^e LUMO = - (4.4 + E_{red}^{onset}) eV.

^f Electrochemical band gap (eV) = HOMO–LUMO; ^g The B3LYP/6-311+G(d,p)/6-31G(d,p) obtained values. ^h Optical band gap energies were calculated from the equation $E_g = hc/\lambda = 1240/\lambda$ eV, where λ is the edge wavelength (in nm) of UV/Vis absorption spectrum.

Table 3a. UV-Vis absorption data (λ_{abs}) of **4a–4c** and **8a–8c** in different solvents.

Compound ^a	Hexane (nm) (ϵ) ^b	CHCl ₃ (nm) (ϵ) ^b	CH ₃ OH (nm) (ϵ) ^b
4a	288(57100), 347(19600), 364(27700), 384(25400)	289(51900), 350(16400), 368(24100), 388(21900)	288(60500), 347(18700), 365(27100), 384(25100)

4b	292(52700), 347(17400), 364(24700), 384(22600)	294(43500), 350(13300), 368(19500), 388(17700)	288(58400), 347(18000), 365(25400), 384(23500)
4c	298(57900), 347(19100), 364(26200), 384(23700)	301(54700), 350(17800), 368(24400), 388(21800)	287(65200), 346(23300), 364(31200), 384(28600)
8a	288(69300), 346(17900), 364(27600), 383(25900)	289(63600), 349(15700), 367(24300), 387(22500)	287(67400), 346(17400), 365(25600), 384(24300)
8b	288(70100), 346(17600), 364(26900), 383(25200)	290(60900), 349(15000), 367(22800), 387(20700)	288(69700), 346(17900), 364(26000), 384(24200)
8c	300(57600), 346(17300), 364(24800), 383(23000)	302(39400), 349(11500), 367(16400), 387(15100)	299(49800), 346(15900), 364(21400), 384(19700)

^a All the compounds measured in 1×10^{-5} M concentration, at room temperature,

^b Molar extinction coefficient (ϵ , $\text{mol}^{-1} \text{cm}^{-1}$).

Table 3b: Simulated UV-Vis absorption data (λ_{abs}) of **4a-4c** and **8a-8c** in different solvents obtained using TDDFT methods at B3LYP/6-311G(d,p) level

Compound	Hexane λ_{max} in nm (f)	CHCl_3 λ_{max} in nm (f)	CH_3OH λ_{max} in nm (f)	CI of wave function ^a
4a	399.41 (0.2163)	400.24 (0.2178)	399.5 (0.204)	H \rightarrow L (0.686) H \rightarrow L+1 (0.137)
4b	398.72 (0.2173)	399.58 (0.2180)	398.9 (0.204)	H \rightarrow L (0.685)

				H → L+1 (0.137)
4c	398.66 (0.2400)	399.45 (0.2441)	398.66 (0.232)	112 → 113 (0.691)
				H → L+1 (0.106)
8a	393.39 (0.1401)	393.83 (0.1440)	392.83 (0.137)	H → L (0.700)
8b	393.84 (0.1401)	394.31 (0.1434)	393.33 (0.134)	H → L (0.699)
8c	393.69 (0.138)	394.19 (0.1388)	393.61 (0.0742)	H → L (0.692)
				H → L+1 (-0.104)

^a CI values given in CHCl₃ (for remaining solvents these values are almost same)

Table 4. Fluorescence data (λ_{em}) of **4a–4c** and **8a–8c** in different solvents and solid state.

Compound ^a	Hexane (nm)	Toluene (nm)	EtOAc (nm)	CHCl ₃ (nm)	CH ₃ CN (nm)	DMF (nm)	CH ₃ OH (nm)	Solid State ^b (nm)	Φ^c
4a	407	415	415	422	426	433	456	451	0.62
4b	408	416	415	421	426	432	453	513	0.68
4c	408	416	414	419	426	428	446	502	0.61
8a	395, 414	398, 419	395, 415	399, 419	398, 415	400, 420	396, 415	444	0.93
8b	394, 413	399, 418	395, 414	398, 418	398, 416	400, 418	396, 415	466	0.92
8c	394, 414	399, 417	395, 414	399, 417	396, 416	400, 418	395, 413	449	0.98

^a All the compounds measured in 1 x 10⁻⁵ M concentration at rt, excitation at 390 nm.

^b Measured in solid state at rt.

^c Fluorescence quantum yields relative to 9,10-diphenyl anthracene ($\Phi = 0.9$ in cyclohexane).

Table 5. Electroluminescent performance data of compounds **4a–4c** and **8a–8c** as emitters.

V_{onset}^b	L_{max}^c	η_c^d	η_p^e	EL λ_{max}	CIE _(x,y)
---------------	-------------	------------	------------	--------------------	----------------------

Device ^a	(V)	(cd m ⁻²)	(cd A ⁻¹)	(lm W ⁻¹)	(nm)	
4a	9.0	160	0.12	0.02	515, 553	0.33, 0.48
4b	12.0	710	0.43	0.06	515	0.25, 0.47
4c	12.0	45	0.05	0.01	515	0.29, 0.44
8a	7.0	1728	0.89	0.20	485, 505	0.22, 0.40
8b	7.0	365	0.62	0.19	515, 553	0.32, 0.42
8c	7.0	547	0.57	0.19	505	0.22, 0.37

^a Device configuration: ITO (120 nm)/ α -NPD (30 nm)/**4a-4c** or **8a-8c** (35 nm)/BCP (6 nm)/ Alq₃ (28 nm)/LiF (1 nm)/Al (150 nm). ^b V_{onset} is defined as applied voltage for determining the luminance of 1 cd m⁻². ^c L_{max} is the maximum luminance. ^d η_c is the maximum current efficiency at applied voltage in parentheses. ^e η_p indicates the maximum power efficiency at applied voltages in parentheses.

Table 6. Electroluminescent performance data of **8a** as an electron transport material.

Device	V_{onset} ^c (V)	L_{max} ^d (cd m ⁻²)	η_c ^e (cd A ⁻¹)	η_p ^f (lm W ⁻¹)	EL λ_{max} (nm)
Alq ₃ ^a	11.0	5810	8.69	1.47	512,545
8a ^b	11.0	5610	11.7	2.05	512,545

^a Device

configuration: ITO (120 nm)/ α -NPD (30 nm)/Ir(ppy)₃ doped CBP (35 nm)/BCP (6 nm)/Alq₃ (28 nm)/LiF (1 nm)/Al (150 nm). ^b Device configuration: ITO (120 nm)/ α -NPD (30 nm)/Ir(ppy)₃ doped CBP (35 nm)/BCP (6 nm)/**8a** (28 nm)/LiF (1 nm)/Al (150 nm). ^c V_{onset} is defined as applied voltage for determining the luminance of 1 cd m⁻². ^d L_{max} is the maximum luminance. ^e η_c is the maximum current efficiency at applied voltage in parentheses. ^f η_p indicates the maximum power efficiency at applied voltages in parentheses.

Table 7. Electroluminescent performance data of **8a** as an electron transport emitter.

Device	$V_{\text{onset}}^{\text{c}}$ (V)	$L_{\text{max}}^{\text{d}}$ (cd m^{-2})	$\eta_{\text{c}}^{\text{e}}$ (cd A^{-1})	$\eta_{\text{p}}^{\text{f}}$ (lm W^{-1})	EL λ_{max} (nm)
8a ^a	3.0	1284	0.71	0.32	485
8a ^b	7.0	300	0.11	0.03	505

^a Device configuration: ITO/F4-TCNQ (2 nm)/ α -NPD (40 nm)/**8a** (50 nm)/LiF (1 nm)/Al (150 nm).

^b Device configuration: ITO/ α -NPD (40 nm)/**8a** (50 nm)/LiF (1 nm)/Al (150 nm). ^c V_{onset} is defined as applied voltage for determining the luminance of 1 cd m^{-2} . ^d L_{max} is the maximum luminance. ^e η_{c} is the maximum current efficiency at applied voltage in parentheses. ^f η_{p} indicates the maximum power efficiency at applied voltages in parentheses.

Design and Synthesis of Novel Anthracene Derivatives as n-type Emitters for Electroluminescent Devices: A Combined Experimental and DFT Study

G. Mallesham,^{a,b} S. Balaiah,^b M. Ananth Reddy,^{a,b} B. Sridhar,^{*c} Punita Singh,^d Ritu Srivastava,^{*d} K. Bhanuprakash^{*b,e} and V. Jayathirtha Rao^{*a,e}

Graphical abstract

Six novel anthracene-oxadiazole derivatives have been designed, synthesized and characterized using various experimental and theoretical studies. The combination of anthracene and oxadiazole moieties helps in development of emitting and electron transporting materials with improved efficiencies for OLEDs.

